Radiative natural supersymmetry: Reconciling electroweak fine-tuning and the Higgs boson mass

Howard Baer, Vernon Barger, Peisi Huang, Dan Mickelson, Azar Mustafayev, and Xerxes Tata

Phys. Rev. D **87**, 115028 — Published 28 June 2013

DOI: 10.1103/PhysRevD.87.115028

Preprint typeset in JHEP style - PAPER VERSION

UH-511-1204-12

Radiative natural supersymmetry: Reconciling electroweak fine-tuning and the Higgs boson mass

Howard Baer[a], **Vernon Barger**[b], **Peisi Huang**[b], **Dan Mickelson**[a], **Azar Mustafayev**[c] **and Xerxes Tata**[c]

[a] *Dept. of Physics and Astronomy, University of Oklahoma, Norman, OK 73019, USA*

[b] *Dept. of Physics, University of Wisconsin, Madison, WI 53706, USA*

[c] *Dept. of Physics and Astronomy, University of Hawaii, Honolulu, HI 96822, USA*

E-mail: baer@nhn.ou.edu, barger@pheno.wisc.edu, phuang7@wisc.edu, mickelso@nhn.ou.edu, azar@phys.hawaii.edu, tata@phys.hawaii.edu

Abstract: Models of natural supersymmetry seek to solve the little hierarchy problem by positing a spectrum of light higgsinos $\lesssim 200-300$ GeV and light top squarks $\lesssim 600$ GeV along with very heavy squarks and TeV-scale gluinos. Such models have low electroweak fine-tuning and satisfy the LHC constraints. However, in the context of the MSSM, they predict too low a value of m_h, are frequently in conflict with the measured $b \to s\gamma$ branching fraction and the relic density of thermally produced higgsino-like WIMPs falls well below dark matter (DM) measurements. We propose a framework dubbed *radiative natural SUSY* (RNS) which can be realized within the MSSM (avoiding the addition of extra exotic matter) and which maintains features such as gauge coupling unification and radiative electroweak symmetry breaking. The RNS model can be generated from SUSY GUT type models with non-universal Higgs masses (NUHM). Allowing for high scale soft SUSY breaking Higgs mass $m_{H_u} > m_0$ leads to *automatic cancellations* during renormalization group (RG) running, and to *radiatively-induced low fine-tuning* at the electroweak scale. Coupled with large mixing in the top squark sector, RNS allows for fine-tuning at the 3-10% level with TeV-scale top squarks and a 125 GeV light Higgs scalar h. The model allows for at least a partial solution to the SUSY flavor, CP and gravitino problems since first/second generation scalars (and the gravitino) may exist in the 10-30 TeV regime. We outline some possible signatures for RNS at the LHC such as the appearance of low invariant mass opposite-sign isolated dileptons from gluino cascade decays. The smoking gun signature for RNS is the appearance of light higgsinos at a linear e^+e^- collider. If the strong CP problem is solved by the Peccei-Quinn mechanism, then RNS naturally accommodates mixed axion-higgsino cold dark matter, where the light higgsino-like WIMPS – which in this case make up only a fraction of the measured relic abundance – should be detectable at upcoming WIMP detectors.

1. Introduction

The recent discovery by Atlas and CMS of a Higgs-like resonance at the CERN LHC[1, 2] adds credence to supersymmetric models (SUSY) of particle physics in that the mass value $m_h \simeq 125$ GeV falls squarely within the narrow window predicted by the Minimal Supersymmetric Standard Model (MSSM): $m_h \sim 115 - 135$ GeV[3]. At the same time, the lack of a SUSY signal at LHC7 and LHC8 implies $m_{\tilde{g}} \gtrsim 1.4$ TeV (for $m_{\tilde{g}} \sim m_{\tilde{q}}$) and $m_{\tilde{g}} \gtrsim 0.9$ TeV (for $m_{\tilde{g}} \ll m_{\tilde{q}}$)[4, 5]. While weak scale SUSY[6] provides a solution[7] to the gauge hierarchy problem via the cancellation of quadratic divergences, the apparently multi-TeV sparticle masses required by LHC searches seemingly exacerbates *the little hierarchy problem* (LHP):

- how do multi-TeV values of SUSY model parameters conspire to yield a Z-boson (Higgs boson) mass of just 91.2 (125) GeV?

Models of *natural supersymmetry*[8] address the LHP by positing a spectrum of light higgsinos $\lesssim 200$ GeV and light top- and bottom-squarks with $m_{\tilde{t}_{1,2},\tilde{b}_1} \lesssim 600$ GeV along with very heavy first/second generation squarks and TeV-scale gluinos[9, 10, 11]. Such a spectrum allows for low electroweak fine-tuning (EWFT) while at the same time keeping sparticles safely beyond LHC search limits. Because third generation scalars are in the few hundred GeV range, the radiative corrections to m_h, which increase logarithmically with $m_{\tilde{t}_i}^2$, are never very large and these models have great difficulty in accommodating a light SUSY Higgs scalar with mass $m_h \sim 125$ GeV [11, 12]. Thus, we are faced with a new conundrum:

- how does one reconcile low EWFT with such a large value of m_h [13]?

A second problem occurs in that

- the predicted branching fraction for $b \to s\gamma$ decay is frequently at odds with the measured value due to the very light third generation squarks[11].

A third issue appears in that

- the light higgsino-like WIMP particles predicted by models of natural SUSY lead to a thermally-generated relic density which is typically a factor 10-15 below[14, 11] the WMAP measured value of $\Omega_{CDM}h^2 \simeq 0.11$.

One solution to the fine-tuning/Higgs problem is to add extra fields to the theory, thus moving beyond the MSSM[13]. For example, adding an extra singlet as in the NMSSM permits a new quartic coupling in the Higgs potential thus allowing for an increased value of m_h[15]. Alternatively, one may add extra vector-like matter to increase m_h while maintaining light top squarks[16]. In the former case of the NMSSM, adding extra gauge singlets may lead to re-introduction of destabilizing

divergences into the theory[17]. In the latter case, one might wonder about the ad-hoc introduction of extra weak scale matter multiplets and how they might have avoided detection. A third possibility, which is presented below, is to re-examine EWFT and to ascertain if there do indeed exist sparticle spectra *within the MSSM* that lead to $m_h \sim 125$ GeV while maintaining modest levels of electroweak fine-tuning.

1.1 Electroweak fine-tuning

One way to evaluate EWFT in SUSY models is to examine the minimization condition from the Higgs sector scalar potential which determines the Z boson mass. (Alternatively, one may examine the mass formula for m_h and arrive at similar conclusions.) Minimization of the one-loop effective potential $V_{\rm tree} + \Delta V$, leads to

$$\frac{M_Z^2}{2} = \frac{m_{H_d}^2 + \Sigma_d^d - (m_{H_u}^2 + \Sigma_u^u)\tan^2\beta}{\tan^2\beta - 1} - \mu^2 \ , \tag{1.1}$$

where Σ_u^u and Σ_d^d are radiative corrections that arise from the derivatives of ΔV evaluated at the minimum. Eq. (1.1) reduces to the familiar tree-level expression[6] for M_Z^2 when radiative correction terms are ignored. As we will discuss in detail below, Σ_u^u and Σ_d^d include contributions, listed in the Appendix, from various particles and sparticles with sizeable Yukawa and/or gauge couplings to the Higgs sector. To obtain a *natural* value of M_Z on the left-hand-side, one would like each term C_i (with $i = H_d,\ H_u,\ \mu$ as well as $\Sigma_u^u(k)$, $\Sigma_d^d(k)$, where k denotes the various contributions to the Σs that we just mentioned) on the right-hand-side to have an absolute value of order $M_Z^2/2$. Noting that all entries in (1.1) are defined at the weak scale, we are led to define the *electroweak fine-tuning parameter*[1] by [20]

$$\Delta_{\rm EW} \equiv max_i \left(C_i\right)/(M_Z^2/2) \ , \tag{1.2}$$

where $C_{H_u} = |-m_{H_u}^2 \tan^2\beta/(\tan^2\beta - 1)|/$, $C_{H_d} = |m_{H_d}^2/(\tan^2\beta - 1)|/$ and $C_\mu = |-\mu^2|$, along with analogous definitions for $C_{\Sigma_u^u(k)}$ and $C_{\Sigma_d^d(k)}$. Low $\Delta_{\rm EW}$ means less fine-tuning. Since C_{H_d} and $C_{\Sigma_d^d(k)}$ terms are suppressed by $\tan^2\beta - 1$, for even moderate $\tan\beta$ values this expression reduces approximately to

$$\frac{M_Z^2}{2} \simeq -(m_{H_u}^2 + \Sigma_u^u) - \mu^2 \ . \tag{1.3}$$

We see that to get low $\Delta_{\rm EW}$ we require $|-m_{H_u}^2| \sim M_Z^2/2$ and $\mu^2 \sim M_Z^2/2$. The question then arises: what is the model and can we find a set of model parameters

[1]Barbieri and Giudice[18] (and, even earlier, Ellis *et al.*[19]) define a fine tuning measure $\Delta_{BG} = max|(a_i/M_Z^2)\partial M_Z^2/\partial a_i|$ for input parameters a_i. Our definition coincides with theirs when M_Z^2 depends linearly on input parameters (such as μ^2, $m_{H_u}^2$ or $m_{H_d}^2$ using electroweak scale parameters) but differs when the parameter dependence is non-linear. For electroweak scale parameters, the non-linear dependence only occurs in the radiative correction terms Σ_u^u and Σ_d^d and in $\tan\beta$.

such that $\Delta_{\rm EW} \sim 1-30$, corresponding to better than $\Delta_{\rm EW}^{-1} = 3\%$ EWFT? Note that $\Delta_{\rm EW}$ depends only on the weak scale parameters of the theory and hence is essentially fixed by the particle spectrum, independent of how superpartner masses arise.

To understand how the underlying framework for superpartner masses may be relevant, consider a model with input parameters defined at some high scale $\Lambda \gg M_{\rm SUSY}$, where $M_{\rm SUSY}$ is the SUSY breaking scale ~ 1 TeV and Λ may be as high as $M_{\rm GUT}$ or even the reduced Planck mass M_P. Then

$$m_{H_u}^2(M_{\rm SUSY}) = m_{H_u}^2(\Lambda) + \delta m_{H_u}^2 \tag{1.4}$$

where

$$\delta m_{H_u}^2 \simeq -\frac{3f_t^2}{8\pi^2}\left(m_{Q_3}^2 + m_{U_3}^2 + A_t^2\right)\log\left(\frac{\Lambda}{M_{\rm SUSY}}\right). \tag{1.5}$$

Requiring $\delta m_{H_u}^2 \leq \Delta \times \frac{m_h^2}{2}$ then leads for $m_h = 125$ GeV to,

$$\sqrt{m_{\tilde{t}_1}^2 + m_{\tilde{t}_2}^2} \lesssim 600 \text{ GeV} \frac{\sin\beta}{\sqrt{1+R_t^2}}\left(\frac{\log\frac{\Lambda}{\rm TeV}}{3}\right)^{-1/2}\left(\frac{\Delta}{5}\right)^{1/2}, \tag{1.6}$$

where $R_t = A_t/\sqrt{m_{\tilde{t}_1}^2 + m_{\tilde{t}_2}^2}$. Taking $\Delta = 10$ and Λ as low as 20 TeV corresponds to[8, 9, 10]

- $|\mu| \lesssim 200$ GeV,
- $m_{\tilde{t}_i},\ m_{\tilde{b}_1} \lesssim 600$ GeV,
- $m_{\tilde{g}} \lesssim 1.5-2$ TeV.

The last of these conditions arises because the squark radiative corrections $\delta m_{\tilde{t}_i}^2 \sim (2g_s^2/3\pi^2)m_{\tilde{g}}^2 \times \log\Lambda$. Setting the log to unity and requiring $\delta m_{\tilde{t}_i}^2 < m_{\tilde{t}_i}^2$ then implies $m_{\tilde{g}} \lesssim 3m_{\tilde{t}_i}$, or $m_{\tilde{g}} \lesssim 1.5-2$ GeV for $\Delta \lesssim 10$. Taking Λ as high as M_{GUT} leads to even tighter constraints: $m_{\tilde{t}_{1,2}}, m_{\tilde{b}_1} \lesssim 200$ GeV and $m_{\tilde{g}} \lesssim 600$ GeV, almost certainly in violation of LHC sparticle search constraints. Since (degenerate) first/second generation squarks and sleptons enter into (1.1) only at the two loop level, these can be much heavier: beyond LHC reach and also possibly heavy enough to provide a (partial) decoupling solution to the SUSY flavor and CP problems. In gravity mediation where $m_{\tilde{q}} \sim m_{3/2}$, then one also solves the cosmological gravitino problem[21, 22] and in GUTs one also suppresses proton decay. Then we may also have

- $m_{\tilde{q},\tilde{\ell}} \sim 10-50$ TeV.

The generic natural SUSY (NS) solution reconciles lack of a SUSY signal at LHC with allowing for electroweak naturalness. It also predicts that the $\tilde{t}_{1,2}$ and $\tilde{b}_1$ may

soon be accessible to LHC searches. New limits from direct top- and bottom-squark pair production searches, interpreted within the context of simplified models, have begun to bite into the NS parameter space[23]. Of course, if $m_{\tilde{t}_{1,2}},\ m_{\tilde{b}_1} \simeq m_{\widetilde{Z}_1}$, then the visible decay products from stop and sbottom production will be soft and difficult to see at the LHC.

A more worrisome problem comes from the newly discovered value of the Higgs mass $m_h \simeq 125$ GeV. In the MSSM, one obtains[3] (assuming that the t-squarks are not very split),

$$m_h^2 \simeq M_Z^2 \cos^2 2\beta + \frac{3g^2}{8\pi^2}\frac{m_t^4}{m_W^2}\left[\ln\frac{m_{\tilde{t}}^2}{m_t^2} + \frac{X_t^2}{m_{\tilde{t}}^2}\left(1-\frac{X_t^2}{12m_{\tilde{t}}^2}\right)\right] \tag{1.7}$$

where $X_t = A_t - \mu\cot\beta$ and $m_{\tilde{t}}^2 \simeq m_{Q_3}m_{U_3}$. For a given $m_{\tilde{t}}^2$, this expression is maximal for large mixing in the top-squark sector with $X_t^{max} = \sqrt{6}m_{\tilde{t}}$. With top-squark masses below about 500 GeV, the radiative corrections to m_h are not large enough to yield $m_h \simeq 125$ GeV even with maximal mixing[13, 11]. This situation has been used to argue that additional multiplets beyond those of the MSSM must be present in order to raise up m_h while maintaining very light third generation squarks[13]. Added to these are the two issues mentioned earlier: 1. the very light third generation squarks[11] endemic to NS lead to a predicted branching fraction for $b \to s\gamma$ decay which is frequently much lower than the measured value[11], and 2. that the relic abundance of higgsino-like WIMPs inherent in NS, calculated in the standard MSSM-only cosmology, is typically a factor 10-15 below measured values[11]. These issues have led to increasing skepticism of weak scale SUSY as realized in the natural SUSY incarnation described above.

A possible resolution to the above issues associated with a NS spectrum is to simply invoke a SUSY particle spectrum at the weak scale (or some other nearby scale[24]), as in the pMSSM model[25] so that large logarithms associated with a high value of Λ are absent. In this case, $\Lambda \sim M_{\rm SUSY}$ and $\delta m_{H_u}^2$ is not enhanced by large logarithms and we may select parameters $m_{H_u}^2 \sim \mu^2 \sim M_Z^2 \sim m_h^2$. Of course, heavy top squarks are needed to obtain the observed value of m_h. While a logical possibility, this solution loses several attractive features of models which are valid up to scales as high as $\Lambda \sim M_{\rm GUT}$, such as gauge coupling unification and radiative electroweak symmetry breaking driven by a large top quark mass.

Another alternative is to use $\Delta_{\rm EW}$ defined above as a fine-tuning measure even for models defined at the high scale. This use of weak scale parameters to define the fine-tuning criterion is a *weaker condition* since it allows for possible cancellations in (1.4). Indeed this is precisely what happens in what is known as the hyperbolic branch or focus point region (HB/FP) of mSUGRA[26]: $m_{H_u}^2(\Lambda) + \delta m_{H_u}^2 \sim m_{H_u}^2(M_{\rm SUSY}) \sim \mu^2 \sim M_Z^2$. The HB/FP region of mSUGRA occurs, however, only for small values of A_0/m_0 [27] and yields $m_h < 120$ GeV, well below the Atlas/CMS measured value of

$m_h \simeq 125$ GeV. Scans over parameter space show that the HB/FP region is nearly excluded if one requires both low $|\mu|$ and $m_h \sim 123 - 127$ GeV [28, 27].

To obtain a viable high scale model we see that we clearly need to go beyond mSUGRA. The small value of $-m_{H_u}^2(M_{SUSY})$ that we require for low EWFT can be obtained in several ways. For instance, we could introduce non-universality of gaugino masses and adopt very high GUT scale values of the $SU(2)$ gaugino mass parameters[29], or a low value of the $SU(3)$ gaugino mass parameter[30]. Both choices would lead to a larger chargino to gluino mass ratio than in models with universal gaugino masses[31], and since charginos couple directly to the Higgs sector, potentially significant contributions to the radiative corrections for gluinos that satisfy the LHC bound. The other way of obtaining small values of $-m_{H_u}^2(M_{SUSY})$ without undue cancellations in (1.1) is to introduce non-universality in the scalar Higgs sector. To facilitate our analysis, we use the two parameter non-universal Higgs mass (NUHM2) extension[32] of the mSUGRA model where $m_{H_u}^2(M_{\rm GUT})$ and $m_{H_d}^2(M_{\rm GUT})$, or equivalently, the weak scale parameters μ and m_A, are chosen independently of matter scalar mass parameters, and the model is completely specified by the parameter set,

$$m_0,\ m_{1/2},\ \mu,\ m_A,\ A_0,\ \tan\beta \qquad \text{(NUHM2)}. \tag{1.8}$$

Modest electroweak fine-tuning is then obtained due to large cancellations between $m_{H_u}^2(\Lambda = M_{\rm GUT})$ and $\delta m_{H_u}^2$.

Along with $-m_{H_u}^2(M_{SUSY}) \sim M_Z^2/2$, low $\Delta_{\rm EW}$ also requires $\mu^2 \sim M_Z^2/2$. In gravity-mediated SUSY breaking models– where the μ problem is solved by the Guidice-Masiero mechanism[33]– one expects that $\mu \sim \lambda m_{3/2}$ where λ is a hidden-visible sector coupling. For small values of λ, then we expect $|\mu| \ll m_{3/2}$ which is then significantly smaller than the typical soft-SUSY breaking masses.

Later in our analysis, we will also allow for the possibility of split matter generations where the third generation mass parameter $m_0(3)$ is independent from the corresponding parameter $m_0(1,2)$ for the first two generations. We refer to this case as the NUHM3 model. The NUHM3 model allows for an improved decoupling solution to the SUSY flavour problem. Finally, we mention that a small magnitude of μ is also possible in the NUHM1 model where we take the two GUT scale Higgs mass parameters to have a common value m_ϕ^2 which can be raised above m_0 until $m_{H_u}^2(M_{\rm SUSY})$ becomes comparable to M_Z^2 [34]. In this case, m_A is of course determined. We consider this case briefly. In all cases, intra-generation splitting is avoided since as noted in Ref. [27], it can lead to large fine-tuning if scalars are very heavy. We emphasize that $\Delta_{\rm EW}$ is determined by physical sparticle masses and couplings so that *our results can be applied to any model that yields a similar spectrum*, irrespective of how sparticles acquire their SUSY breaking mass.

At this point the reader may legitimately wonder about the validity of using $\Delta_{\rm EW}$ as a measure of fine-tuning in the NUHM2 model which is, by construction,

assumed to be a description of physics up to energy scales as large as $M_{\rm GUT}$. The introduction of the $\Delta_{\rm HS}$ in Ref. [27] was precisely to include the impact of these large logarithms – which also appear in (1.6) – on the fine-tuning. The use of $\Delta_{\rm EW}$ as a fine-tuning measure allows for the possibility of large cancellation between $m^2_{H_{u,d}}(\Lambda)$ and the term $\delta m^2_{H_{u,d}}$ (which may include large logarithms). For instance, special regions of parameter space of some models (*e.g.* focus-point SUSY, the mixed-modulus-anomaly-mediation model for special values of the ratio α [35] or particular regions of parameter space of non-universal Higgs mass models) enjoy nearly complete cancellations between the terms with large logarithms and $m^2_{H_{u,d}}(\Lambda)$. In a more encompassing framework that includes the origin of soft SUSY breaking parameters, such cancellations might not only be allowed, but might be automatic [35, 36]. We note, however, that $\Delta_{\rm HS}$, as we have defined it, does *not* take such a cancellation into account; under these circumstances $\Delta_{\rm EW}$ is the appropriate fine-tuning measure to use.

The fine-tuning measure $\Delta_{\rm EW}$ introduced in Ref's. [20] and [27] has several attractive features that merit consideration.

- *Model independent* (within the context of models which reduce to the MSSM at the weak scale): $\Delta_{\rm EW}$ is essentially determined by the sparticle spectrum[27], and – unlike $\Delta_{\rm HS}$ and other measures of fine-tuning – does not depend on the mechanism by which sparticles acquire masses. Since $\Delta_{\rm EW}$ is determined only from weak scale Lagrangian parameters, the phenomenological consequences which may be derived by requiring low Δ_{EW} will apply not only for the NUHM2 model considered here, but also for other possibly more complete (or less complete, such as pMSSM) models which lead to look-alike spectra at the weak scale.

- *Conservative*: $\Delta_{\rm EW}$ captures the minimal fine-tuning that is necessary for any given sparticle spectrum, and so leads to the *most conservative conclusions* regarding fine-tuning considerations.

- *Measureable*: $\Delta_{\rm EW}$ is in principle measurable in that it can be evaluated if the underlying weak scale parameters can be extracted from data.

- *Unambiguous*: Fine-tuning measures which depend on high scale parameter choices, such as the Barbieri-Guidice measure $\Delta_{\rm BG}$ discussed previously, are highly sensitive to exactly which set of model input parameters one adopts: for example, it is well-known that significantly different values of $\Delta_{\rm BG}$ result depending on whether the high scale top-Yukawa coupling is or is not included as an input parameter[37]. There is no such ambiguity in the fine-tuning sensitivity as measured by both $\Delta_{\rm EW}$ and $\Delta_{\rm HS}$.

- *Predictive*: While $\Delta_{\rm EW}$ is less restrictive than Δ_{HS}, it still remains highly restrictive. The requirement of low Δ_{EW} highly disfavors models such as mSUGRA/CMSSM[27], while allowing for very distinct predictions from more general models such as NUHM2.

- *Falsifiable*: The most important prediction from requiring low Δ_{EW} is that $|\mu|$ cannot be too far removed from M_Z. This implies the existence of light higgsinos $\sim 100-300$ GeV which are hard to see at hadron colliders, but which are easily detected at a linear e^+e^- collider with $\sqrt{s} \gtrsim 2|\mu|$. If no higgsinos appear at ILC1000, then the idea of electroweak naturalness in SUSY models is dead.

- *Simple to calculate*: $\Delta_{\rm EW}$ is extremely simple to encode in sparticle mass spectrum programs, even if one adopts models with very large numbers of input parameters.

To illustrate how a low value of $m_{H_u}^2(M_{\rm SUSY})$ is obtained, in Fig. 1 we show the running of various SUSY parameters versus the renormalization scale Q for the RNS2 benchmark point from Ref. [20]. The RNS2 point has parameters $m_0 = 7025$ GeV, $m_{1/2} = 568.3$ GeV, $A_0 = -11426.6$ GeV, $\tan\beta = 8.55$ with $\mu = 150$ GeV and $m_A = 1000$ GeV. The gaugino and matter scalar mass parameters evolve from $m_{1/2}$ and m_0 to their weak scale values, resulting in a pattern of masses very similar to that in mSUGRA. The parameter μ hardly evolves, and for such a low value of $\tan\beta$, $m_{H_d}^2$ also suffers little evolution. Of most interest to us here is the RG evolution of $m_{H_u}^2$. As is well known, the SUSY breaking parameters $m_{Q_3}^2$, $m_{U_3}^2$ and $m_{H_u}^2$ of the scalar fields that couple via the large top quark Yukawa coupling are driven down with reducing values of the scale Q. The reduction is the greatest for $m_{H_u}^2$ which, in fact, is driven negative, triggering the radiative breakdown of electroweak symmetry [38]. We see from the figure that the weak scale value of $-m_{H_u}^2$ has a magnitude $\sim M_Z^2$, and is much smaller than the weak scale value of other mass parameters. This is not an accident because *the NUHM2 model provides us the flexibility to adjust the GUT scale value of $m_{H_u}^2$ so that it barely runs to negative values at the weak scale.* Since $m_{H_u}^2$ is driven radiatively to $\sim -M_Z^2$ at the weak scale, this scenario has been dubbed *Radiative Natural SUSY*, or RNS for short.

In Fig. 2 we scan over parameter space of the NUHM2 model – while enforcing $m_h = 125 \pm 2$ GeV and LHC sparticle mass limits – and plot the value of $\Delta_{\rm HS}$ versus the high scale matter scalar mass parameter m_0. We see that the smallest value of $\Delta_{\rm HS}$ is 10^3 for the lowest values of m_0 allowed. This is because of the large logarithms that we discussed above. The NUHM2 would be fine-tuned to at least 0.1%, and usually even higher fine-tuning is necessary. We will see below that much smaller values of $\Delta_{\rm EW}$ are possible in some parts of parameter space. An underlying high-scale theory that automatically leads to an NUHM2-like spectrum in this parameter

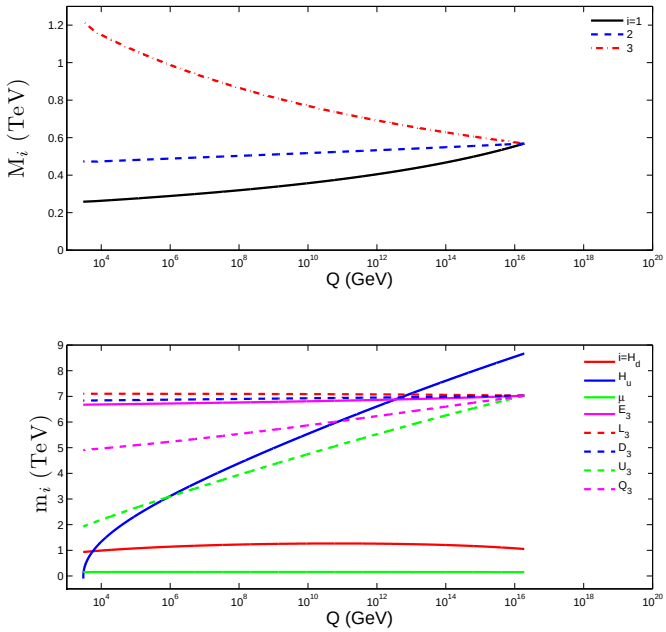

Figure 1: Evolution of SSB parameters from $M_{\rm GUT}$ to M_{weak} for the RNS2 benchmark point taken from in Ref. [20] whose parameters are given in the text. The graph extends to values below $Q^2 = m_{\tilde{t}_1} m_{\tilde{t}_2}$ where the Higgs mass parameters are extracted.

region would then not be so fine-tuned. In contrast, there are no analogous regions of mSUGRA/CMSSM parameters for which we have shown that $\Delta_{\rm EW} \gtrsim 100$[27].

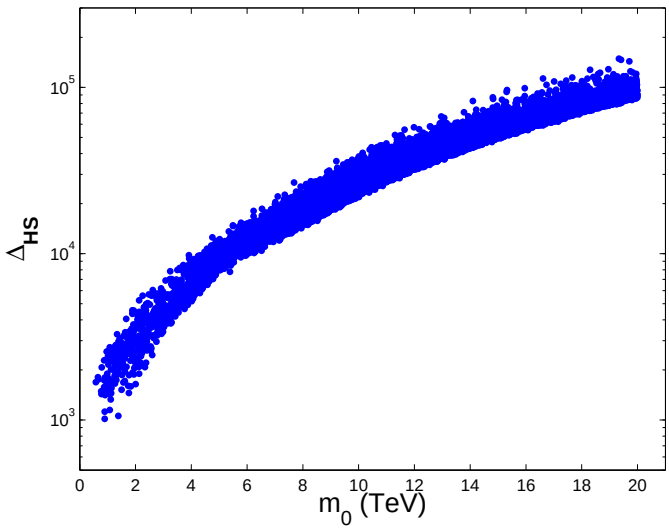

Figure 2: Plot of $\Delta_{\rm HS}$ versus m_0 from a scan over NUHM2 model parameters, accepting only points where $m_h = 125 \pm 2$ GeV and which obey LHC sparticle mass constraints.

In the remainder of this paper, we will explore what parameter choices lead to low values of $\Delta_{\rm EW}$. While Δ_{EW} seems bounded from below by about 100 in mSUGRA/CMSSM[27], we will find that Δ_{EW} as low as ~ 10 can be obtained in NUHM2. In addition, requiring low $\Delta_{EW} \lesssim 30$ places strong restrictions on the allowed sparticle mass spectra, leading to distinctive predictions for collider and dark matter searches.

1.2 Radiative natural supersymmetry

Motivated by the possibility of cancellations occurring in $m_{H_u}^2(M_{\rm SUSY})$, we return to the EWSB minimization condition (1.1) which was introduced earlier, and examine more carefully the radiative corrections embodied in Σ_u^u and Σ_d^d that we have not discussed up to now. These affect the minimization condition in an important way when $m_{H_u}^2(m_{\rm SUSY})$ and μ^2 are much smaller than the scale of other weak scale SUSY breaking parameters. At the one-loop level, Σ_u^u contains the contributions[39, 40] $\Sigma_u^u(\tilde{t}_{1,2})$, $\Sigma_u^u(\tilde{b}_{1,2})$, $\Sigma_u^u(\tilde{\tau}_{1,2})$, $\Sigma_u^u(\widetilde{W}_{1,2})$, $\Sigma_u^u(\widetilde{Z}_{1-4})$, $\Sigma_u^u(h,H)$, $\Sigma_u^u(H^{\pm})$, $\Sigma_u^u(W^{\pm})$, $\Sigma_u^u(Z)$, and $\Sigma_u^u(t)$. Σ_d^d contains similar terms along with $\Sigma_d^d(b)$ and $\Sigma_d^d(\tau)$ while $\Sigma_d^d(t)=0$. The complete set of one-loop contributions to these is listed in the Appendix. There are additional contributions from first/second generation sparticles from their D-term couplings to Higgs scalars. If these squarks, and separately sleptons, are degenerate then these contributions cancel within each generation because the sum of weak isospins/hypercharges of squarks/sleptons total to zero[27]. In the parameter space region where RNS is realized, *i.e.* where $-m_{H_u}^2(M_{\rm SUSY}) \sim \mu^2 \sim M_Z^2$, the radiative correction terms from Σ_u^u may give the largest contributions to $\Delta_{\rm EW}$.

The largest of the Σ_u^u terms almost always come from top squarks for which we find,

$$\Sigma_u^u(\tilde{t}_{1,2}) = \frac{3}{16\pi^2}F(m_{\tilde{t}_{1,2}}^2)\times\left[f_t^2 - g_Z^2 \mp \frac{f_t^2A_t^2 - 8g_Z^2(\frac{1}{4}-\frac{2}{3}x_W)\Delta_t}{m_{\tilde{t}_2}^2 - m_{\tilde{t}_1}^2}\right] \qquad (1.9)$$

where $\Delta_t = (m_{\tilde{t}_L}^2 - m_{\tilde{t}_R}^2)/2 + M_Z^2\cos 2\beta(\frac{1}{4}-\frac{2}{3}x_W)$, $g_Z^2 = (g^2+g'^2)/8$, $x_W \equiv \sin^2\theta_W$ and $F(m^2) = m^2\left(\log(m^2/Q^2)-1\right)$, with $Q^2 = m_{\tilde{t}_1}m_{\tilde{t}_2}$. In Ref. [20], it is shown that for the case of the $\tilde{t}_1$ contribution, as $|A_t|$ gets large there is a suppression of $\Sigma_u^u(\tilde{t}_1)$ due to a cancellation between terms in the square brackets of Eq. (1.9). The $\tilde{t}_2$ contribution is suppressed if there is a sizeable splitting between $m_{\tilde{t}_2}$ and $m_{\tilde{t}_1}$ due to a large cancellation within $F(m_{\tilde{t}_2}^2)$ because $\log(m_{\tilde{t}_2}^2/Q^2) = \log(m_{\tilde{t}_2}/m_{\tilde{t}_1}) \simeq 1$. The large $|A_t|$ values suppress both top squark contributions to Σ_u^u, and at the same time lift up the value of m_h, which is near maximal for large negative A_t. Combining all effects, one sees that the same mechanism responsible for boosting the value of m_h into accord with LHC measurements can also suppress the Σ_u^u contributions to EWFT, leading to a model with low EWFT.

To display the quality of EWFT explicitly, we show in Fig. 3*a* the various *signed* contributions to $M_Z^2/2$ that enter Eq. (1.1) for the RNS2 point from Fig. 1

and Ref. [20]. In this figure, we label these signed contributions by C_i where $i = H_u, H_d, \mu, \Sigma_u^u, \Sigma_d^d$. The largest contributions come from $C_{\Sigma_u^u} \sim 0.04$ TeV^2 and $C_{H_u} \sim -0.03$ TeV^2. In frame b), we show these same quantities for the mSUGRA model (where μ and m_A are outputs instead of input parameters). Here, the maximal contributions $C_{H_u} \sim 15$ TeV^2 and $C_\mu \sim -15$ TeV^2. Frame c) compares results from the two models using a common scale. Here, it is clearly seen that the mSUGRA model is enormously fine-tuned compared to the RNS2 benchmark point.

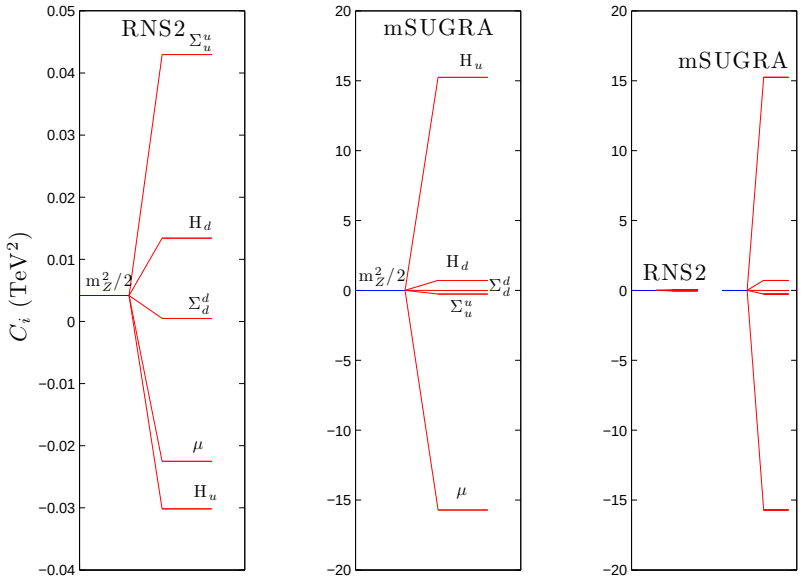

Figure 3: Signed contributions to $M_Z^2/2$ from terms in the EWSB minimization condition Eq. 1.1 from a) the RNS2 benchmark point defined in the text and b) the corresponding mSUGRA model as RNS2 with μ and m_A as outputs rather than inputs. In frame c), the results for both models are plotted on a common scale.

Our goal in this paper is to provide a rather complete characterization of radiative natural SUSY. This should provide a comprehensive picture as to where in model parameter space we can find 1) $m_h \sim 125$ GeV along with 2) low EWFT $\Delta_{\rm EW} \lesssim 30$ while at the same time 3) respecting LHC constraints on sparticle masses. With this goal in mind, in Sec. 2 we show parameter space regions leading to low $\Delta_{\rm EW}$ from scans over the 2-parameter non-universal Higgs model NUHM2 which allow for radiative natural SUSY. In Sec. 3 we extend the results to include the split generation non-universal Higgs model NUHM3, wherein high scale third generation scalar masses $m_0(3)$ need not equal first/second generation scalar masses $m_0(1,2)$. While the former implementation allows for fewer parameters, the additional freedom in the NUHM3 model allows for a more robust decoupling solution to the SUSY flavor and CP problems because heavier multi-TeV first/second generation sfermion masses

are then possible. In Sec. 4, we show that constraints from B-physics – especially $BF(b \to s\gamma)$ are much more easily respected in RNS than in generic NS models. In Sec. 5, we discuss prospects for detecting RNS at the LHC. We also show the new RNS m_0 *vs.* $m_{1/2}$ parameter plane, which offers a template for future searches for RNS at the LHC. Searches for RNS at the ILC are discussed in Sec. 6 while direct and indirect detection of higgsino-like WIMPs is discussed in Sec. 7. In an Appendix, we present formulae needed for implementation of our measure of electroweak fine-tuning $\Delta_{\rm EW}$.

2. Radiative natural SUSY from the NUHM models

The direct supersymmetrization of the Standard Model – augmented by weak scale soft supersymmetry breaking terms – leads to the Minimal Supersymmetric Standard Model (MSSM). Since the mass scale of the MSSM is stable to radiative corrections even when the MSSM is embedded into a high scale framework, it is tempting to speculate that the MSSM arises as the low energy limit of an underlying SUSY grand unified theory with a unification scale $M_{\rm GUT} \simeq 2\times 10^{16}$ GeV. Indeed, the MSSM (possibly with additional gauge singlets and/or additional complete $SU(5)$ multiplets) receives some indirect support from experiment in that 1) the measured weak scale gauge couplings nearly unify at $M_{\rm GUT}$ under MSSM RG evolution, 2) radiative corrections due to the large top quark Yukawa coupling – consistent with $m_t \sim 173$ GeV – dynamically breaks electroweak symmetry, and 3) a light SM-like Higgs boson has been discovered to be lying squarely within the narrow mass window predicted by the MSSM.

Motivated by these successes, the interesting question arises as to whether a natural SUSY sparticle mass spectrum, *i.e.* one with a modest value of $\Delta_{\rm EW}$, can be consistently generated from a model with parameters defined at the high scale $Q = M_{\rm GUT}$. Naturalness requires $|\mu| \sim M_Z\sqrt{\Delta_{\rm EW}/2}$, whilst the recently measured[41] value of the branching fraction $BF(B_s \to \mu^+\mu^-)$ qualitatively agrees with the predicted SM value, which in turn requires the CP odd boson A to be relatively heavy. We are thus led to adopt the 2-parameter non-universal Higgs model (NUHM2)[32], wherein weak scale values of μ and m_A may be used as inputs in lieu of GUT scale values of $m_{H_u}^2$ and $m_{H_d}^2$.[2] In Sec. 2.1, for simplicity we take a common GUT scale mass parameter m_0 for *all* the matter scalars. Motivated by Grand Unification, we also assume a common GUT scale gaugino mass parameter. Later in Sec. 3 we also explore the possibility of split first/second versus third generation matter scalars where we allow the third generation GUT scale mass parameter $m_0(3)$ to differ from $m_0(1,2)$ for the first/second generation scalars. Universality within each

[2]Since the Higgs fields belong to different multiplets from matter fields, it is easy to envisage models with independent SUSY breaking mass parameters for Higgs and matter scalars.

generation is well-motivated by $SO(10)$ GUT symmetry, since all matter multiplets of a single generation belong to a 16-dimensional spinor rep of $SO(10)$. We can also envisage some degree of non-universality between $m_0(1)$ and $m_0(2)$ as long as both lie in the tens of TeV regime: such a scenario invokes a partial decoupling-partial degeneracy solution to the SUSY flavor and CP problems (for constraints from FCNC processes [42], see *e.g.* Ref. [43]). For convenience, we will take $m_0(1) = m_0(2)$.

2.1 RNS from the NUHM2 model

The NUHM2 model is defined by the NUHM2 parameter set (1.8) introduced earlier. We take $m_t = 173.2$ GeV throughout this paper. For our calculations, we use the Isajet 7.83 [44] SUSY spectrum generator Isasugra[45]. Isasugra begins the calculation of the sparticle mass spectrum with input $\overline{DR}$ gauge couplings and f_b, f_τ Yukawa couplings at the scale $Q = M_Z$ (f_t running begins at $Q = m_t$) and evolves the 6 couplings up in energy to scale $Q = M_{\rm GUT}$ (defined as the value Q where $g_1 = g_2$) using two-loop RGEs. We do not enforce the exact unification condition $g_3 = g_1 = g_2$ at $M_{\rm GUT}$, since a few percent deviation from unification can be attributed to unknown GUT-scale threshold corrections [46]. Next, we use the SSB boundary conditions at $Q = M_{\rm GUT}$ and evolve the set of 26 coupled two-loop MSSM RGEs [47, 48] back down in scale to $Q = M_Z$. Full two-loop MSSM RGEs are used for soft term evolution, and the gauge and Yukawa coupling evolution includes threshold effects in the one-loop beta-functions, so the gauge and Yukawa couplings transition smoothly from the MSSM to SM effective theories as different mass thresholds are passed. In Isasugra, the values of SSB terms which mix are frozen out at the scale $Q = M_{\rm SUSY} = \sqrt{m_{\tilde{t}_L} m_{\tilde{t}_R}}$, while non-mixing SSB terms are frozen out at their own mass scale [45]. The scalar potential is minimized using the RG-improved one-loop MSSM effective potential evaluated at an optimized scale $Q = M_{\rm SUSY}$ to account for leading two-loop effects [49]. Once the tree-level sparticle mass spectrum is obtained, one-loop radiative corrections are calculated for all sparticle and Higgs boson masses, including complete one-loop weak scale threshold corrections for the top, bottom and tau masses at scale $Q = M_{\rm SUSY}$ [50]. Since Yukawa couplings are modified by the threshold corrections, the solution must be obtained iteratively, with successive up-down running until a convergence at the required level is found. Since Isasugra uses a "tower of effective theories" approach to RG evolution, we expect a more accurate evaluation of the sparticle mass spectrum for models with split spectra than with programs such as SuSpect, SoftSUSY or Spheno, which make an all-at-once transition from the MSSM to SM effective theories.

Our goal in this section is to find parameter ranges of the NUHM2 model which satisfy LHC sparticle and Higgs boson mass constraints while maintaining a low level of EWFT. We will also calculate the allowed mass range for various sparticles in low fine-tuned/phenomenologically viable parameter space. Toward this end, we search for regions of the NUHM2 parameter space with $\Delta_{\rm EW} \lesssim 30$, where fine-tuning is

better than about 3%. We will also require that our calculated light Higgs scalar mass lies within the range $m_h = 125 \pm 2$ GeV to allow for an estimated uncertainty in our calculation of m_h. We will also require that the parameters m_0 and $m_{1/2}$ respect the recent LHC limits on squark and gluino masses obtained within the mSUGRA model [4, 5].

We search for radiative Natural SUSY solutions by first performing a random scan over the following NUHM2 parameter ranges:

$$\begin{aligned} m_0 &: 0 - 20 \text{ TeV}, \\ m_{1/2} &: 0.3 - 2 \text{ TeV}, \\ -3 < A_0/m_0 &< 3, \\ \mu &: 0.1 - 1.5 \text{ TeV}, \\ m_A &: 0.15 - 1.5 \text{ TeV}, \\ \tan\beta &: 3 - 60. \end{aligned} \tag{2.1}$$

We require of our solutions that:

- electroweak symmetry be radiatively broken (REWSB),
- the neutralino $\widetilde{Z}_1$ is the lightest MSSM particle,
- the light chargino mass obeys the model independent LEP2 limit, $m_{\widetilde{W}_1} > 103.5$ GeV[51],
- LHC search bounds on $m_{\tilde{g}}$ and $m_{\tilde{q}}$ are respected,
- $m_h = 125 \pm 2$ GeV.

To begin our investigation of NUHM2 model parameters leading to low $\Delta_{\rm EW}$, in Fig. 4 we plot each scan point as a red "+" in frames of $\Delta_{\rm EW}$ versus *a*) m_0, *b*) $m_{1/2}$, *c*) A_0/m_0, *d*) $\tan\beta$, *e*) μ, and *f*) m_A. Since low $\Delta_{\rm EW}$ solutions are only possible for low values of μ, we have performed a separate narrow scan, but this time with μ restricted between 100–300 GeV. The results of this second scan is shown by the blue crosses in the figure.

We see from the plots that $\Delta_{\rm EW}$ varies from as low as ~ 10 ($\Delta_{EW}^{-1} = 10\%$ EWFT) to over 1000. While the bulk of points shown are fine-tuned with large $\Delta_{\rm EW} \gtrsim 100$, there do exist many solutions with $\Delta_{\rm EW} \lesssim 30$, corresponding to better than 3% EWFT. The RNS solutions with $\Delta_{\rm EW} \lesssim 30$ are obtained for values of $m_0 \sim 1 - 8$ TeV. In the cases where m_0 is as high as 5-10 TeV, the top squark masses are driven to much lower values via 1) the large top-quark Yukawa coupling f_t which suppresses top-squark soft masses during RG evolution, 2) large mixing effects which can suppress $m_{\tilde{t}_1}$ and yield a large $m_{\tilde{t}_1} - m_{\tilde{t}_2}$ splitting, and 3) two-loop RGE suppression of diagonal top squark mass terms arising from large first/second

generation sfermion masses[52, 53, 54]. If m_0 is too large – in this case above $\sim$ 10 TeV – then these suppression mechanisms are insufficient to drive $m_{\tilde{t}_{1,2}}$ to low enough values to allow for low EWFT. Thus, the span of points shown in frame *a*) trends upward in $\Delta_{\rm EW}$ as m_0 increases past about 8 TeV. We also see that for the red pluses in frame *a*) $\Delta_{\rm EW}$ has an upper bound close to about 500 if $m_0 \lesssim 10$ TeV. For still larger values of m_0 then $\Delta_{\rm EW}$ increases with m_0. This is because while μ^2 (or equivalently $-m_{H_u}^2$) is the largest of the quantities in (1.1) for the lower range of m_0, for very large values of m_0 then Σ_u^u begins to dominate. The blue crosses from the narrow scan with small μ have a different shape from the red broad scan since the upper edge is mostly determined by Σ_u^u, and so increases with m_0.

In frame *b*) of Fig. 4, we show $\Delta_{\rm EW}$ *vs.* $m_{1/2}$. Here, the low values of $\Delta_{\rm EW}$ span a wide range of $m_{1/2}$ values from $0.3-1.5$ TeV. Since $m_{\tilde{g}} \sim (2.5-3)m_{1/2}$, we expect $\Delta_{\rm EW} \lesssim 30$ for $m_{\tilde{g}}$ values up to about 4 TeV. For the entire parameter space (red pluses) $\Delta_{\rm EW}$ is roughly evenly distributed with respect to the gaugino mass parameter. In frame *c*), we show $\Delta_{\rm EW}$ *vs.* A_0/m_0. We see a clear trend for low values of EWFT when $|A_0/m_0| \sim 1.5-2$. The reason is that the hole at low magnitudes of A_0/m_0 and small values of $\Delta_{\rm EW}$ occurs because of the Higgs mass constraint. Large magnitudes of GUT scale A_0 lead to correspondingly large weak scale A_t parameters, which, in turn, provide large mixing in the top-squark sector. This leads to low EWFT and also heightened values of $m_h \sim 125$ GeV. Frame *d*) shows $\Delta_{\rm EW}$ *vs.* $\tan\beta$. We see a slight preference for low $\tan\beta \sim 10-20$ but otherwise no structure to speak of. Frame *e*) shows $\Delta_{\rm EW}$ versus the weak scale value of μ. The parabolic lower edge of the span of points reflects the upper bound on μ necessary for low EWFT. From the plot, bounds on μ can be conveniently read off: for instance, requiring $\Delta_{\rm EW} \lesssim 30$ then requires $\mu \lesssim 350$ GeV. Of course, models with low $\mu \sim 100$ GeV but multi-TeV top squarks can still be very fine-tuned if the dominant contributions to $\Delta_{\rm EW}$ arise from $\Sigma_u^u(\tilde{t}_i)$. In frame *f*), we plot $\Delta_{\rm EW}$ *vs.* m_A. We see that low $\Delta_{\rm EW}$ can be found over the entire range of $m_A \sim 0.15-1.5$ TeV, so this parameter is not so relevant towards achieving low EWFT.

Next, to gain a sense of the sparticle mass ranges expected from RNS, we plot $\Delta_{\rm EW}$ versus selected sparticle masses. First, since $m_0 \sim 2-8$ TeV for $\Delta_{\rm EW} \lesssim 30$, we expect first and second generation squark and slepton masses also within this range (which is for the most part inaccessible LHC SUSY searches). Next, in frame *a*) of Fig. 5, we show $\Delta_{\rm EW}$ *vs.* $m_{\tilde{g}}$. We find that requiring $\Delta_{\rm EW} \lesssim 30$ requires $m_{\tilde{g}} \sim 1-4$ TeV. The lower portion of this range should be accessible to LHC14 searches, while the upper part lies beyond any LHC luminosity upgrade[55].

In frame *b*), we show $\Delta_{\rm EW}$ versus the lighter top squark mass $m_{\tilde{t}_1}$. Here, we see that $\Delta_{\rm EW} \lesssim 30$ allows $m_{\tilde{t}_1} \sim 0.5-2.5$ TeV range. This is well above the range expected in generic NS models[9, 10], where $m_{\tilde{t}_{1,2}}$ has been advocated to lie below about 600 GeV. In frame *c*), we show $\Delta_{\rm EW}$ *vs.* $m_{\tilde{t}_2}$. Here, we find that $m_{\tilde{t}_2}$ can range up to ~ 6 TeV for $\Delta_{\rm EW} \lesssim 30$. Such high values of $m_{\tilde{t}_2}$ are helpful to increase

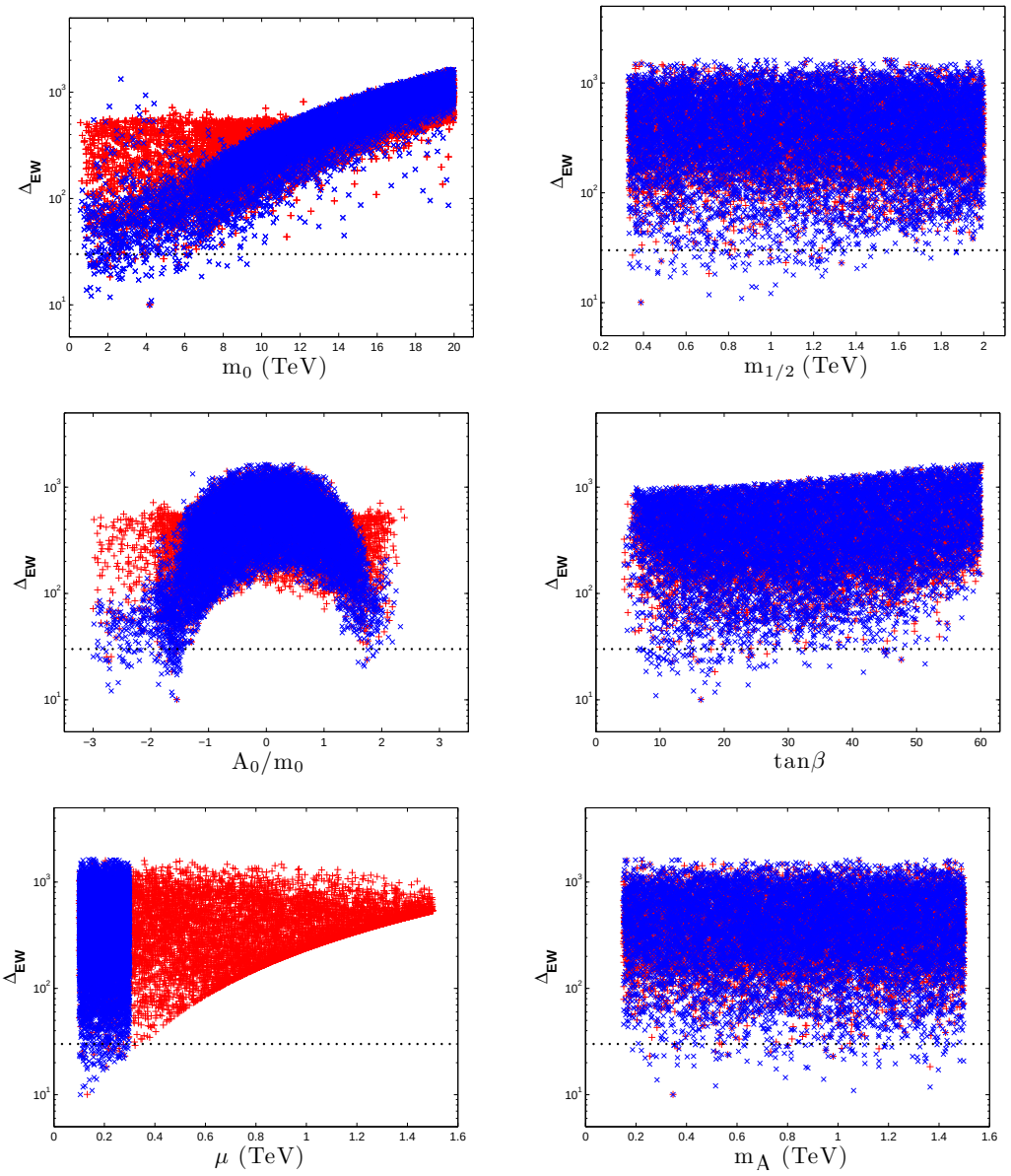

Figure 4: The dependence of $\Delta_{\rm EW}$ on various NUHM2 parameters from a scan (2.1) over parameter space (red pluses) and for the dedicated scan with 100 GeV$< \mu <$300 GeV (blue crosses). The line at $\Delta_{\rm EW} = 30$ is to guide the eye.

radiative corrections to the light Higgs mass m_h into the 125 GeV range. However, such heavy top squarks lie far beyond any conceivable LHC reach. In frame *d*), we show $\Delta_{\rm EW}$ *vs.* $m_{\tilde{b}_1}$. Here we see $m_{\tilde{b}_1} \sim 0.8-6$ TeV, which again allows for far heavier bottom squarks than previous NS models, where $m_{\tilde{t}_{1,2}}$ and $m_{\tilde{b}_1}$ all were suggested to be $\lesssim 600$ GeV.

In Fig. 6*a*), we show $\Delta_{\rm EW}$ *vs.* $m_{\widetilde{W}_1}$. For RNS models, $m_{\widetilde{W}_1} \simeq m_{\widetilde{Z}_{1,2}} \sim |\mu|$, *i.e.* its mass is roughly equal to that of the two lighter neutralinos. Since $\widetilde{W}_1$ is mainly

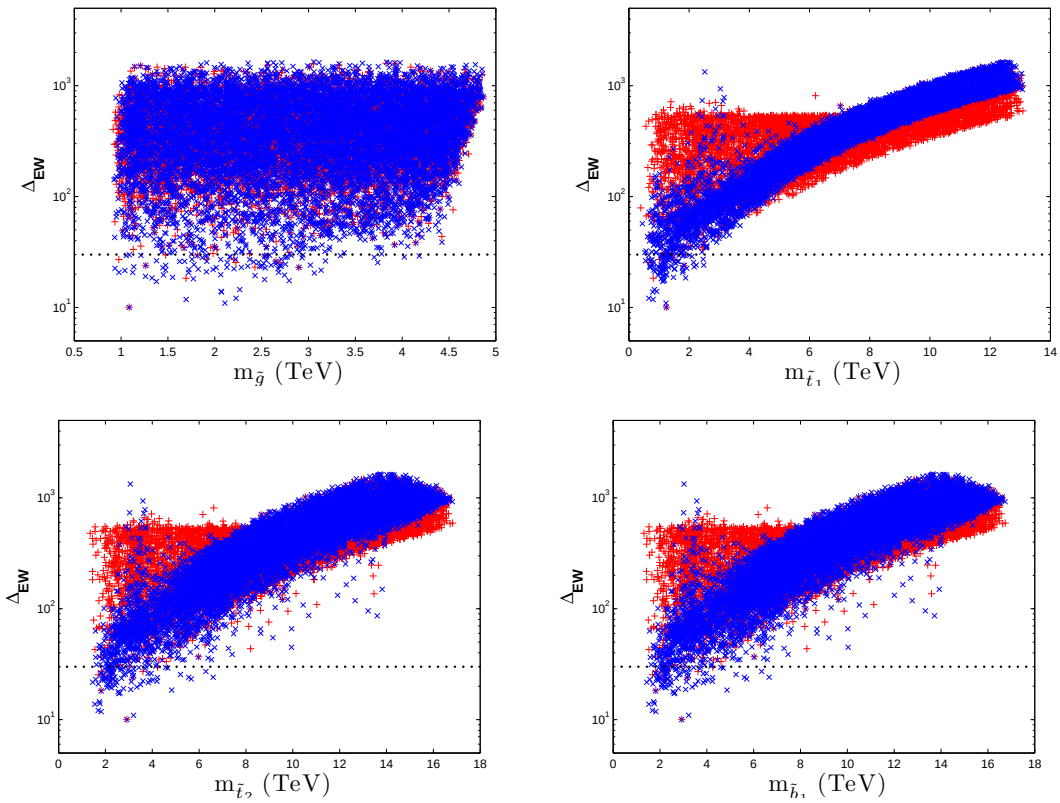

Figure 5: The value of $\Delta_{\rm EW}$ versus gluino and third generation squark masses from a scan over NUHM2 parameter space. As in Fig. 4, the red pluses denote the distributions from the complete scan, whereas the blue crosses depict the results for the dedicated low μ scan. The line at $\Delta_{\rm EW} = 30$ is to guide the eye.

higgsino-like near the lower edge of the envelope of points, the distribution follows a similar pattern as for the $\Delta_{\rm EW}$ *vs.* μ plot in Fig. 4. We see that for $\Delta_{\rm EW} \lesssim 20$, $m_{\widetilde{W}_1} \lesssim 250$ GeV. Thus, a linear collider operating with $\sqrt{s} > 2m_{\widetilde{W}_1}$ will *directly probe* the lowest (and hence most lucrative!) values of $\Delta_{\rm EW}$ if the relatively soft visible daughters of the chargino can be distinguished over two-photon backgrounds[56]. In this sense, it has been emphasized that for models of natural SUSY, a linear e^+e^- collider would be a higgsino factory in addition to a Higgs factory[14, 11, 20]! In frame *b*), we show $\Delta_{\rm EW}$ *vs.* $m_{\widetilde{W}_2}$. In the RNS model, the $\widetilde{W}_2$ is nearly pure wino-like and its mass can range between $\sim 0.3 - 1.2$ TeV for $\Delta_{\rm EW} \lesssim 30$. Since RNS as presented here includes gaugino mass unification, then typically $\widetilde{Z}_{1,2}$ are higgsino-like, $\widetilde{Z}_3$ is bino-like and $\widetilde{Z}_4$ is wino-like. Since the $SU(2)$ gauge coupling g is rather large, we expect significant rates for $\widetilde{W}_2^{\pm}\widetilde{Z}_4$ production at LHC, at least for the lower portion of the range of $m_{\widetilde{W}_2}$. In frame *c*), we show the $m_{\widetilde{Z}_2} - m_{\widetilde{Z}_1}$ mass difference in RNS versus $\Delta_{\rm EW}$. For most points with $\Delta_{\rm EW} \lesssim 30$, we find that $m_{\widetilde{Z}_2} - m_{\widetilde{Z}_1} \lesssim 10 - 20$ GeV. Some points with $\Delta_{\rm EW} \sim 30 - 40$ have a mass difference

as large as 100 GeV; these points arise from sampling the lower portion of the $m_{1/2}$ range, which gives rise to gaugino masses comparable in magnitude to $|\mu|$ so that the lighter electroweakinos are actually gaugino-higgsino mixtures. For the more likely small mass gap case, the lighter neutralinos are dominantly higgsino-like and decay via $\widetilde{Z}_2 \to \widetilde{Z}_1 f\bar{f}$ (here f denotes SM-fermions) through the virtual Z. Then decays into opposite-sign same-flavor (OS/SF) isolated dileptons should occur at $\sim 3\%$ for each charged lepton species. The presence of low invariant mass OS/SF isolated dileptons from boosted $\widetilde{Z}_2$ produced in gluino or gaugino cascade decay events could then be a distinctive signature of RNS at the LHC. For NUHM2 models with larger values of $\Delta_{\rm EW}$, falling outside the RNS low EWFT requirement, $m_{\widetilde{Z}_2}$ can be greater than $m_{\widetilde{Z}_1} + M_Z$ or $m_{\widetilde{Z}_1} + m_h$ so that two body decays of $\widetilde{Z}_2$ are then allowed. Finally, in frame *f*), we show $\Delta_{\rm EW}$ *vs.* m_h. Here, we see the lower $m_h \sim 123-124$ GeV values are just slightly preferred by EWFT over the higher range, although values of m_h as high as ~ 126.5 GeV occur for $\Delta_{\rm EW} = 30$.

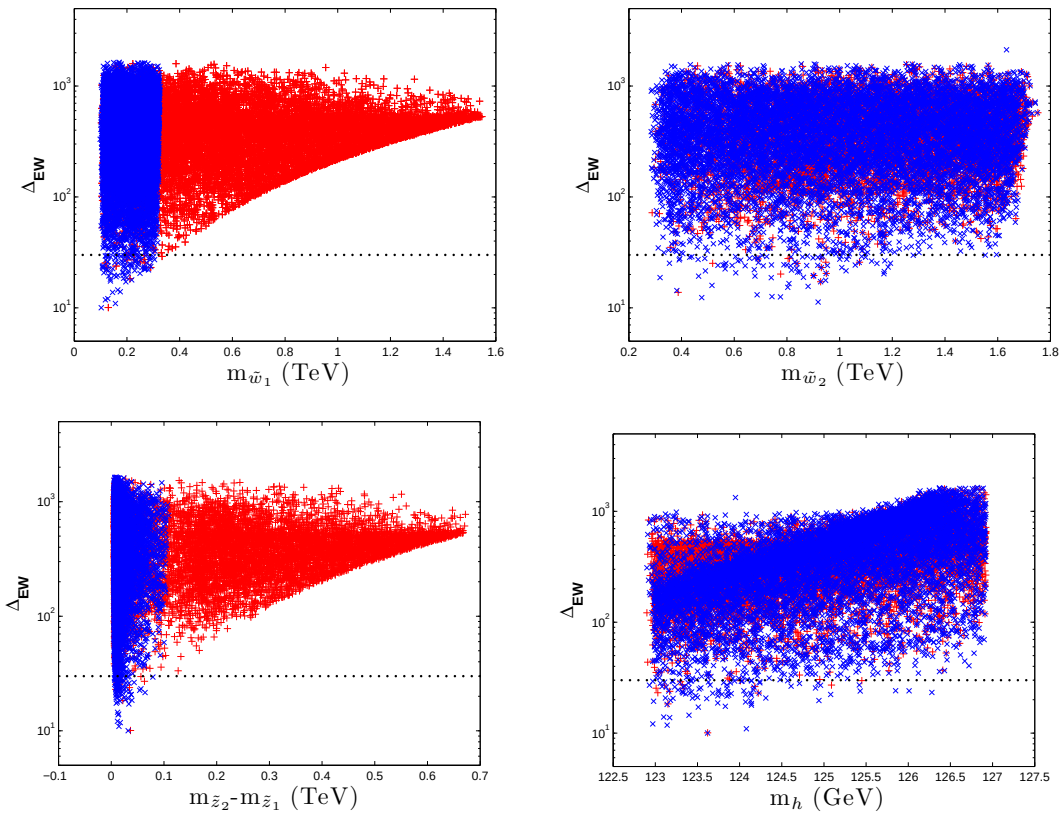

Figure 6: The value of $\Delta_{\rm EW}$ versus electroweak -ino and Higgs boson masses from a scan over NUHM2 parameter space. As in Fig. 4, the red pluses denote the distributions from the complete scan, whereas the blue crosses depict the results for the dedicated low μ scan. The line at $\Delta_{\rm EW} = 30$ is to guide the eye.

While our methodology allows one to find a low value of μ^2 for any value of m_0

and $m_{1/2}$, this by itself does not guarantee a small value of $\Delta_{\rm EW}$. In addition, the GUT scale value of $m_{H_u}^2$ has to be adjusted very precisely to obtain low EWFT, which could be viewed as a different sort of fine-tuning: that only a very narrow range of $m_{H_u}^2(M_{\rm GUT})$ values will yield $-m_{H_u}^2 \sim M_Z^2$ at the weak scale.[3] This can be seen from Table 1 where we plot the value of $m_{H_u}^2(M_{\rm GUT})$ which is needed to generate small μ solutions for two different cases of NUHM2 model parameters. Optimistically speaking, we would view this as essentially determining the GUT scale value of $m_{H_u}^2/m_0^2$ to be very nearly 1.65 (Case A) or 1.71 (Case B). It is gratifying to see that the GUT scale values of *all* scalar mass parameters have no hierarchy as expected in models of gravity-mediated SUSY breaking where all scalar masses might be expected to be comparable at the high scale.

Case A			**Case B**		
$m_{H_u}^2(M_{\rm GUT})$	μ	$\Delta_{\rm EW}$	$m_{H_u}^2(M_{\rm GUT})$	μ	$\Delta_{\rm EW}$
1.03×10^7	150	9.04	2.73×10^7	150	15.4
1.02×10^7	250	18.8	2.72×10^7	250	24.1
1.00×10^7	400	42.4	2.70×10^7	400	49.5

Table 1: An illustration of the sensitivity of the EWFT fine-tuning measure $\Delta_{\rm EW}$ to $m_{H_u}^2(M_{\rm GUT})$. For case **A** the NUHM2 parameters are $m_0 = 2.5$ TeV, $m_{1/2} = 400$ GeV, $\tan\beta = 10$, $m_A = 1$ TeV, while for case **B** we have, $m_0 = 4$ TeV, $m_{1/2} = 1$ TeV, $\tan\beta = 15$, $m_A = 2$ TeV. For both cases, we take $A_0 = -1.6m_0$. The numbers in the Table are in GeV units.

To be more general, we show in Fig. 7 a scatter plot of $\Delta_{\rm EW}$ versus the GUT scale ratio $m_{H_u}^2/m_0$ from our scan over NUHM2 models. We find that for points with $\Delta_{\rm EW} \lesssim 30$, then $m_{H_u}(M_{\rm GUT}) \sim (1-2)m_0$.

2.2 RNS from the NUHM1 model?

Up to this point we have focused on RNS from the NUHM2 model. However, it is of interest to see if low EWFT is also possible within the NUHM1 [32] framework in which H_u and H_d have equal GUT scale mass parameters; *i.e.* $m_{H_u}^2(M_{\rm GUT}) = m_{H_d}^2(M_{\rm GUT}) \equiv m_\phi^2$. As mentioned above, m_ϕ^2 is then adjusted to that $m_{H_u}^2(M_{\rm SUSY}) \sim M_Z^2$. For brevity, we confine our investigation to model lines where we fix m_0, $m_{1/2}$ and A_0 to be the same as for the RNS2 model point, but where we vary m_ϕ, the common GUT scale Higgs mass parameter and $\tan\beta$. In Fig. 8 we show the value of *a)* μ, *b)* m_A, and *c)* $\Delta_{\rm EW}$ versus m_ϕ for $\tan\beta = 8.85$ (the RNS2 value), 25, 40 and 50. We see that the various curves in frame *a)* are quite close (except at very large values where they dive down). This is essentially because the top Yukawa coupling that

[3]From the perspective introduced in Sec. 1, we would look for an underlying model where $m_{H_u}^2$ is thus determined.

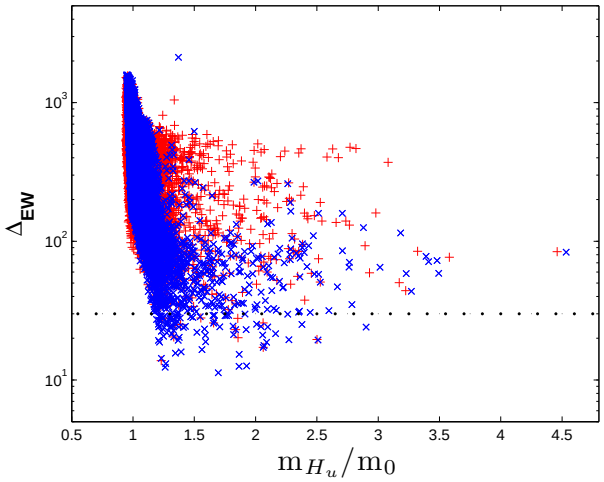

Figure 7: The value of $\Delta_{\rm EW}$ versus $m_{H_u}/m_0(M_{\rm GUT})$ from the scan over the NUHM2 parameter space. As before, the red pluses are for the scan over the entire range of μ while the blue crosses are for the dedicated scan with μ limited to the 100-300 GeV range. The line at $\Delta_{\rm EW}=30$ is to guide the eye.

dominantly affects $m_{H_u}^2$ (remember that $m_{H_u}^2(M_{\rm SUSY})$ determines μ) hardly varies with $\tan\beta$; the small differences arise from the (subdominant) effects of bottom Yukawa couplings. In contrast, the m_A values in frame b) reduce considerably as $\tan\beta$ increases. We can understand this if we remember that the bottom Yukawa coupling– which increases with $\tan\beta$– drives $m_{H_d}^2$ to low values thus reducing $m_A^2\simeq m_{H_d}^2+\mu^2$ for larger $\tan\beta$ values. Turning to frame c) we see that for this model line with $\tan\beta=8.55$ (uppermost curve), $\Delta_{\rm EW}$ reduces with increasing m_ϕ as in the μ curve in frame a) until the kink at which it starts increasing. We have checked that the kink occurs when μ^2 becomes so low that the $m_{H_d}^2$ term becomes larger than all other terms in (1.1). For larger values of $\tan\beta$, the $m_{H_d}^2$ contribution is suppressed, resulting in smaller values of $\Delta_{\rm EW}$. However, in none of the cases shown does $\Delta_{\rm EW}$ drop below ~ 80. It may be a useful exercise to scan the NUHM1 parameter space to see just how small the EWFT can be when all LHC constraints are satisfied.

3. RNS from the NUHM3 (split generation) model

In this Section, we investigate if any advantage can be gained for RNS models if we allow for a splitting between scalars of the third generation and those of the first/second generations. We adopt the parameter set

$$m_0(1,2),\ m_0(3),\ m_{1/2},\ A_0,\ \tan\beta,\ \mu,\ m_A \qquad \text{(NUHM3)} \tag{3.1}$$

where $m_0(3)$ is the GUT scale third generation soft SUSY breaking mass parameter

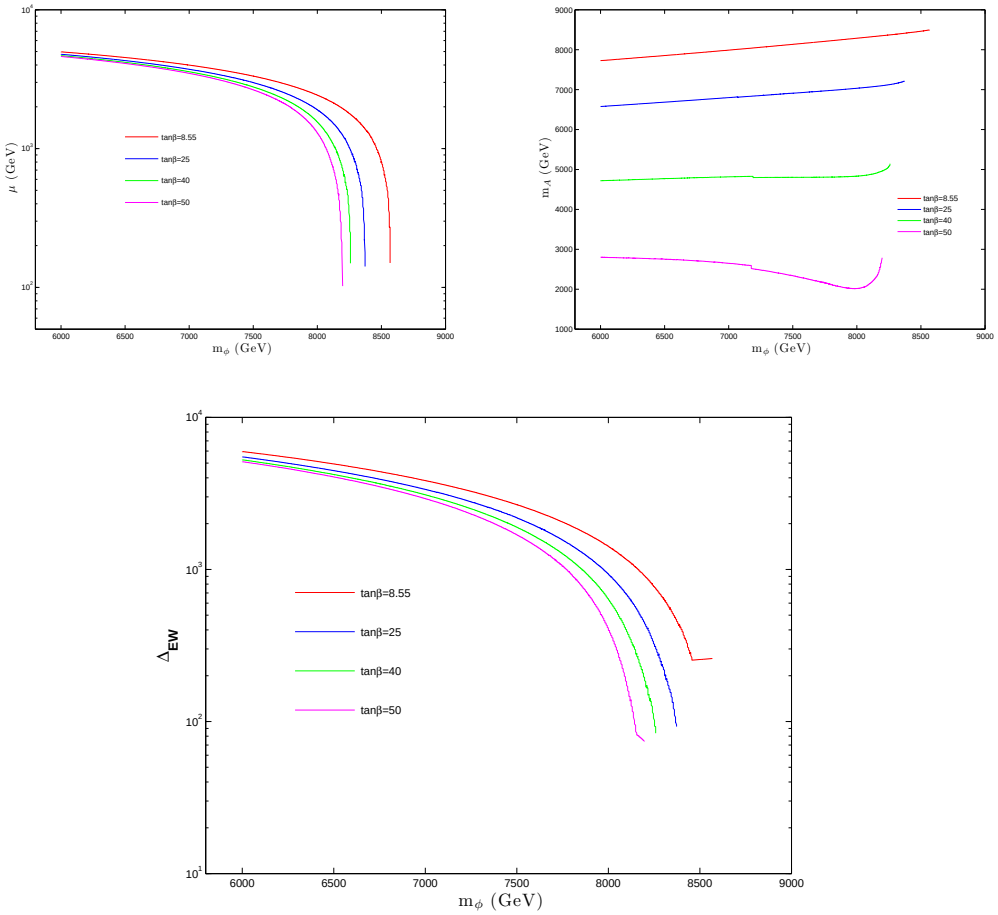

Figure 8: Plot of *a*) μ, *b*) m_A and *c*) $\Delta_{\rm EW}$ in the 1-parameter NUHM1 model versus m_ϕ for RNS2 model parameters $m_0 = 7025$ GeV, $m_{1/2} = 568.3$ GeV, $A_0 = -11426.6$ GeV and for several values of $\tan\beta$. In all the frames the order of the lines is that of increasing $\tan\beta$, with $\tan\beta = 8.55$ on the top and $\tan\beta = 50$ on the bottom.

and $m_0(1,2)$ is the corresponding (common) parameter for the first/second generation.

We search again for RNS solutions from the split generation parameter space by implementing a random scan over the parameters:

$$\begin{aligned} m_0(3) &: 0 - 20 \text{ TeV}, \\ m_0(1,2) &: m_0(3) - 30 \text{ TeV}, \\ m_{1/2} &: 0.3 - 2 \text{ TeV}, \\ -3 < A_0/m_0 &< 3, \\ \mu &: 0.1 - 1.5 \text{ TeV}, \\ m_A &: 0.15 - 1.5 \text{ TeV}, \\ \tan\beta &: 3 - 60. \end{aligned} \tag{3.2}$$

We implement the same LHC sparticle mass and $m_h = 125 \pm 2$ GeV constraints as before.

In Fig. 9, we show $\Delta_{\rm EW}$ versus $m_0(3)$ and also versus $m_0(1,2)$. The results for $\Delta_{\rm EW}$ versus other parameters are very similar to Fig. 4 so we do not repeat them here. From Fig. 9*a*), we see that RNS solutions with $\Delta_{\rm EW} \lesssim 30$ can be found for $m_0(3)$ values ranging between 1-8 TeV, similar to results found in Fig. 4 for the NUHM2 model. It is interesting to note that the smallest values of $\Delta_{\rm EW}$ in the figure are no smaller than for the NUHM2 model. The gap at small values of $m_0(3)$ is an artifact of the upper limit on $m_{1/2}$ in our scan: for small values of $m_0(3)$ the lighter t-squark is often driven to tachyonic masses by two-loop contributions of heavy first/second generation squarks. We have checked that with larger values of $m_{1/2}$ in the scan, solutions fill in the entire gap. Again, even though the GUT scale value of $m_0(3)$ is in the multi-TeV regime, the $\tilde{t}_2$ and especially $\tilde{t}_1$ physical masses are considerably lower – in the few TeV regime – due to radiative effects from RGE running and also large mixing.

The key advantage of the NUHM3 model is seen in Fig. 9*b*), where we plot $\Delta_{\rm EW}$ versus $m_0(1,2)$. In this case, we see that GUT scale first/second generation scalar masses can easily range between $1-30$ TeV while still maintaining low $\Delta_{\rm EW}$. The solutions with $m_0(1,2)$ in the multi-TeV region will also produce first/second generation squark and slepton masses which are comparable to $m_0(1,2)$. This allows for a much more robust solution to the SUSY flavor/CP problems. It also ameliorates the cosmological gravitino problem if $m_{3/2} \sim m_0(1,2)$ as is expected in simple models of gravity-mediation.

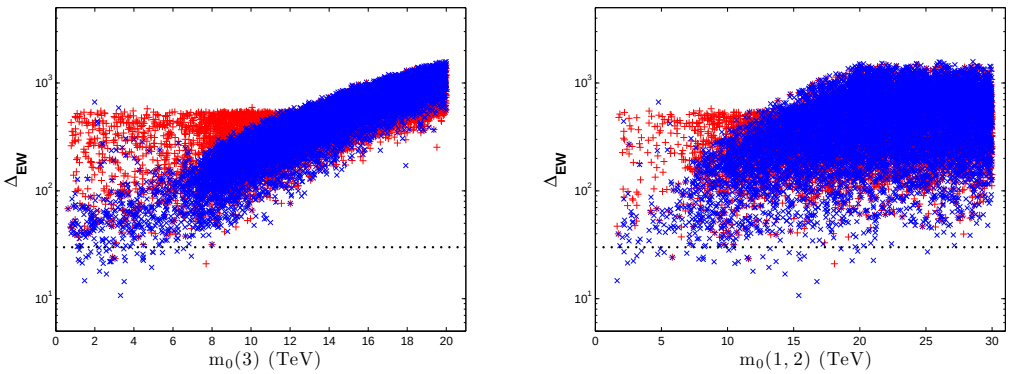

Figure 9: The value of $\Delta_{\rm EW}$ versus $m_0(3)$ and $m_0(1,2)$ from a scan over NUHM3 model with split first/second and third generations. As in Fig. 4, the red pluses denote the distributions from the complete scan, whereas the blue crosses depict the results for the dedicated low μ scan. The line at $\Delta_{\rm EW} = 30$ is to guide the eye.

We do not show plots of $\Delta_{\rm EW}$ versus sparticle masses since these are very similar to results shown in Fig. 5 and Fig. 6 except for the fact that NUHM3 scans allow

for much heavier first/second generation squark and slepton masses in the 10-30 TeV range, whereas in the NUHM2 model the squarks and sleptons are typically constrained to be below 8 TeV due to the imposed relation $m_0(3) = m_0(1,2)$.

4. Rare B decay constraints on RNS

4.1 BF($b \to s\gamma$)

The combination of several measurements of the $b \to s\gamma$ decay rate finds that $BF(b \to s\gamma) = (3.55 \pm 0.26) \times 10^{-4}$ [57]. This is slightly higher than the SM prediction[58] of $BF^{SM}(b \to s\gamma) = (3.15 \pm 0.23) \times 10^{-4}$. SUSY contributions to the $b \to s\gamma$ decay rate come mainly from chargino-stop loops and the W-charged Higgs loops, and so are large when these particles are light and when $\tan\beta$ is large[59]. Thus, in generic natural SUSY where $m_{\tilde{t}_{1,2},\tilde{b}_1} \lesssim 500$ GeV, one finds generally large deviations from the SM value for $BF(b \to s\gamma)$, as shown in Ref. [11]. In contrast, in radiative natural SUSY where third generation squarks are in the TeV range, SUSY contributions to $BF(b \to s\gamma)$ are more suppressed. The situation is shown in Fig. 10a) along with the measured central value (green solid line) and errors. The red points all have $\Delta_{\rm EW} < 30$ and qualify as RNS points. We see the bulk of RNS points are consistent with the measured $BF(b \to s\gamma)$, although there are outliers.

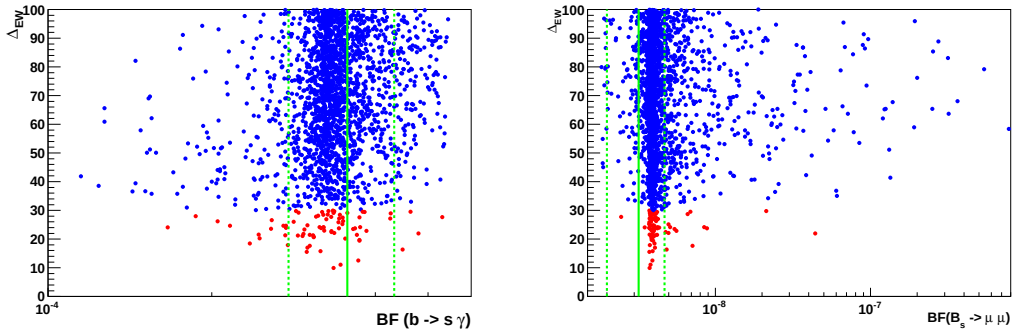

Figure 10: The values of $\Delta_{\rm EW}$ versus a) $BF(b \to s\gamma)$ and b) $BF(B_s \to \mu^+\mu^-)$. The vertical lines represent the experimental measurements with uncertainties.

4.2 $B_s \to \mu^+\mu^-$

Recently, the LHCb collaboration has discovered an excess over the background for the decay $B_s \to \mu^+\mu^-$[41]! They find a branching fraction of $BF(B_s \to \mu^+\mu^-) = 3.2^{+1.5}_{-1.2} \times 10^{-9}$ in accord with the SM prediction of $(3.2 \pm 0.2) \times 10^{-9}$[60]. In supersymmetric models, this flavor-changing decay occurs through pseudoscalar Higgs A exchange[61], and the contribution to the branching fraction from SUSY is proportional to $\frac{(\tan\beta)^6}{m_A^4}$. We show the value of $BF(B_s \to \mu^+\mu^-)$ from RNS in Fig. 10b). The

decay is most constraining at large $\tan\beta \sim 50$ as occurs in Yukawa-unified models[62] and low m_A. In the case of RNS with lower $\tan\beta$ and heavier m_A, the constraint is less important. The bulk of the RNS points in Fig. 10*b*) fall well within the newly measured error bands although there are some outlier red points, mainly at larger values of the branching fraction.

4.3 $(g-2)_\mu$

In addition, the well-known $(g-2)_\mu$ anomaly has been reported as a roughly 3σ deviation from the SM value: $\Delta a_\mu = (28.7 \pm 8.0) \times 10^{-10}$[63]. In RNS, since the $\tilde{\mu}_{1,2}$ and $\tilde{\nu}_\mu$ masses are expected to be in the multi-TeV range, only a tiny non-standard contribution to the $(g-2)_\mu$ anomaly is expected, and alternative explanations for this anomaly would have to be sought.

5. RNS at LHC

Here we list a few of the possibilities for an LHC search for radiative natural SUSY. A thorough study of signal and background simulations will be presented in an upcoming study [64].

The hallmark feature of radiative natural SUSY models is the presence of light higgsino states $\widetilde{W}_1$ and $\widetilde{Z}_{1,2}$ with masses $\sim |\mu| \sim 100-300$ GeV, and usually a small mass gap $m_{\widetilde{W}_1} - m_{\widetilde{Z}_1}$ and $m_{\widetilde{Z}_2} - m_{\widetilde{Z}_1}$ of order 10-30 GeV with a possible exception of low $m_{1/2}$ and larger μ where there can be substantial gaugino-higgsino mixing.

One possibility for RNS at LHC is to search for clean trilepton events from $\widetilde{W}_1\widetilde{Z}_2$ production followed by $\widetilde{W}_1 \to \widetilde{Z}_1\ell\nu_\ell$ and $\widetilde{Z}_2 \to \widetilde{Z}_1\ell^+\ell^-$ decays where $\ell = e$ or μ. This signal has been investigated in Ref. [14]. There, the $p_T(\ell)$ values were typically found to be quite low in the 5-15 GeV range making detection difficult. The small mass difference between the parent and daughter neutralino will also mean that the invariant mass of the opposite-sign same-flavor dilepton pair will be small, making it more challenging to separate it from SM origins. Nevertheless, this reaction certainly motivates an LHC search for clean trilepton states with very soft lepton p_T values, as low as is experimentally feasible.

While first/second generation squarks are expected to be in the multi-TeV range, the value of $m_{\tilde{g}}$ is expected to be $\sim 1-5$ TeV. The lower portion of this mass range $m_{\tilde{g}} \sim 1-2$ TeV should be accessible to LHC searches for gluino pair production $pp \to \tilde{g}\tilde{g}$. For RNS models, since $m_{\tilde{t}_{1,2}} \ll m_{\tilde{q}}$, then gluino three-body decays to third generation particles typically dominate: $\tilde{g} \to tb\widetilde{W}_1$ or $t\bar{t}\widetilde{Z}_i$. Thus, we would expect $\tilde{g}\tilde{g}$ events to contain up to four b-jets, and 2-4 reconstructable top quarks. A small fraction of events would contain $\widetilde{Z}_2 \to \widetilde{Z}_1\ell^+\ell^-$ where $m(\ell^+\ell^-)$ is bounded by $m_{\widetilde{Z}_2} - m_{\widetilde{Z}_1} \sim 10-20$ GeV. Normally the leptons from $\widetilde{Z}_2$ decay would be rather soft, but in the case of large boosts from the gluino cascade decay, the opposite-sign/same-flavor pair would be highly collimated in opening angle. We expect LHC14 with 100

fb^{-1} to be able to probe $m_{\tilde{g}} \sim 1-2$ TeV via $\tilde{g}$ cascade decays using analyses similar to those used for gluino searches in mSUGRA when m_0 is very large. [55].

A novel search for RNS at LHC is to look for pair production of the *heavier* gaugino states $\widetilde{W}_2$ and $\widetilde{Z}_3$ and $\widetilde{Z}_4$. Wino pair production occurs via the large $SU(2)$ gauge couplings and leads to large rates for $\widetilde{W}_2\widetilde{Z}_4$ and $\widetilde{W}_2\widetilde{W}_2$ processes. The decays $\widetilde{W}_2 \to W\widetilde{Z}_{1,2}, Z\widetilde{W}_1$ and $\widetilde{Z}_4 \to W\widetilde{W}_1, Z\widetilde{Z}_{1,2}$ occur with significant branching fractions and yield a variety of diboson final states that include spectacular $W^{\pm}W^{\pm}$ and WZ [65] plus $E_T^{\rm miss}$ events with soft debris from the decays of higgsinos. Events with light Higgs bosons instead of gauge bosons in the final state are also possible [66].

As with the mSUGRA model, a wide range of RNS signatures for LHC can be found by exploring the m_0 *vs.* $m_{1/2}$ plane. This plane will look quite different from the mSUGRA case since now we will require small $\mu \sim 100-200$ GeV in accord with EWFT and also $A_0 \sim -1.6m_0$ in accord with $m_h = 125$ GeV and low EWFT. We show the plane in Fig. 11 for $\mu = 150$ GeV with $A_0 = -1.6m_0$, $\tan\beta = 10$ and $m_A = 1$ TeV. Here, we plot contours $m_h = 123$ and 125 GeV and also contours of $\Delta_{\rm EW} = 6$, 10, 15 and 50. Almost the entire plane has low $\Delta_{\rm EW} < 50$, with $5.5 \leq \Delta_{\rm EW} \lesssim 10$ in the lower left portion. In addition, the right-hand portion of the plane has $m_h \gtrsim 123-125$ GeV. The purple-shaded region marked LEP2 has $m_{\widetilde{W}_1} < 103.5$ GeV in violation of LEP2 limits on chargino pair production. We also show recent LHC constraints from gluino/squark searches within the mSUGRA model as the black contour.[4] We extrapolate those constraints to much higher m_0 values via the dashed black contour. Over the entire plane, $m_{\widetilde{W}_1} \sim m_{\widetilde{Z}_{1,2}} \sim \mu = 150$ GeV so there would always be light higgsino pair production at LHC. The region with $m_{1/2} \lesssim 0.6$ TeV yields $m_{\tilde{g}} \lesssim 2$ TeV and should be accessible to future gluino pair production searches. Signals from wino pair production may also be observable at the LHC, and perhaps even at LHC8, if the heavier chargino is sufficiently light.

6. RNS at ILC

Since the main feature of RNS models is the presence of light higgsinos $\widetilde{W}_1$, $\widetilde{Z}_1$ and $\widetilde{Z}_2$, we expect excellent prospects for testing RNS at a linear e^+e^- collider. Pair production for charged higgsinos via the reaction $e^+e^- \to \widetilde{W}_1^+\widetilde{W}_1^-$ would yield soft but observable decay products from $\widetilde{W}_1 \to \widetilde{Z}_1 f\bar{f}'$ decay, where f and f' are SM fermions. These decay products should be easily detectable in the clean environment of e^+e^- colliders, and moreover should be acollinear in the transverse plane as opposed to two-photon backgrounds $\gamma\gamma \to f\bar{f}$ where visible decay products tend to come out

[4]Strictly speaking, these are the constraints obtained in the mSUGRA model for $A_0 = 0$ from the non-observation of signals from gluino and first generation squark production. Since the masses of these sparticles depend mostly on m_0 and $m_{1/2}$, it is reasonable to suppose these also apply to the plane in Fig. 11.

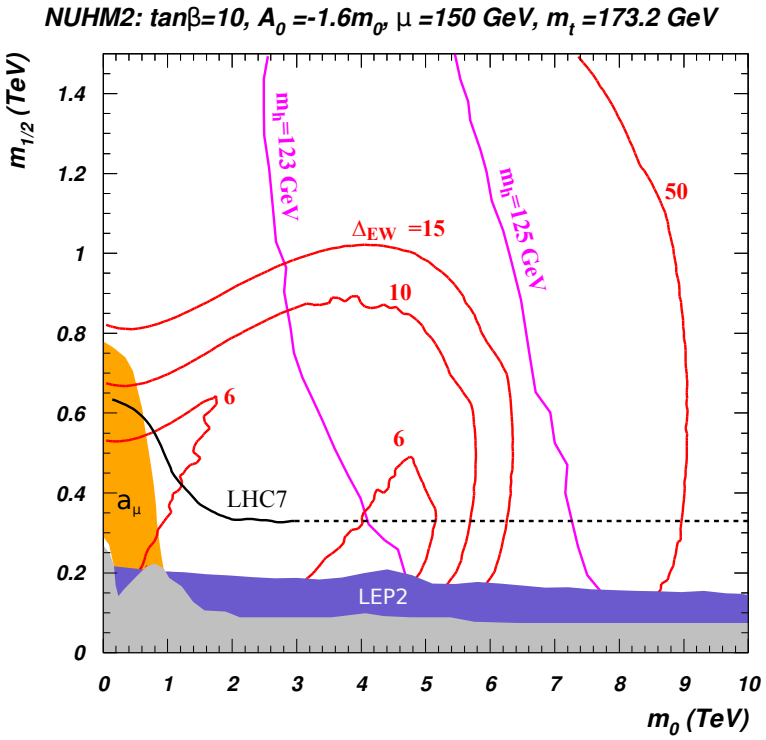

Figure 11: Contours of $\Delta_{\rm EW}$ (red curves) and m_h (purple curves) in the m_0 versus $m_{1/2}$ plane of RNS model with $A_0 = -1.6m_0$, $\tan\beta = 10$, $\mu = 150$ GeV and $m_A = 1$ TeV.

back-to-back. The entire m_0 *vs.* $m_{1/2}$ plane shown in Fig. 11 will be accessible to an ILC with $\sqrt{s} \gtrsim 2m_{\widetilde{W}_1} \simeq 2|\mu|$.

Moreover, the cross section for the reaction $e^+e^- \to \widetilde{Z}_1\widetilde{Z}_2$ should also be large and provide corroborative evidence. These cross sections will have a distinctive shape versus beam polarization as shown in Ref. [14] which should be indicative of higgsino pair production. We note here that since $E_{CM} \gtrsim 2m_{\widetilde{W}_1} \sim 2|\mu|$, and $\Delta_{\rm EW} \sim \mu^2/(M_Z^2/2)$, then an e^+e^- collider with a CM energy E_{CM} directly probes

$$\Delta_{\rm EW} \sim E_{CM}^2/(2M_Z^2)\,, \tag{6.1}$$

so that even a low energy e^+e^- linear collider would probe the most lucrative regions of RNS parameter space (that portion with lowest $\Delta_{\rm EW}$) and as E_{CM} increases, would discover natural SUSY or increasingly exclude it.

7. Search for higgsino-like WIMPs from RNS

One of the distinctive features of natural SUSY models is that the lightest MSSM particle is a higgsino-like neutralino $\widetilde{Z}_1$. If R-parity is conserved, then the $\widetilde{Z}_1$ may make up all or at least a portion of the dark matter in the universe. Higgsinos with mass $m_{\widetilde{Z}_1} > m_W,\ M_Z$ have high annihilation rates into vector boson pairs. Thus, if

they are present in thermal equilibrium in the early universe, then the higgsino relic density may be computed approximately as

$$\Omega_{\widetilde{Z}_1}^{\rm th} h^2 = \frac{s_0}{\rho_c/h^2}\left(\frac{45}{\pi g_*}\right)^{1/2}\frac{x_f}{m_{Pl}}\frac{1}{\langle\sigma v\rangle} \tag{7.1}$$

where s_0 is the entropy density of the universe at the present time, ρ_c is the critical closure density, h is the scaled Hubble constant, g_* is the number of relativistic degrees of freedom at freeze-out, $x_f \sim 25$ is the scaled freeze-out temperature, m_{Pl} is the Planck mass and $\langle\sigma v\rangle$ is the thermally averaged neutralino annihilation cross section times relative velocity. Higgsino-like WIMPs couple with gauge strength to vector bosons so that $\langle\sigma v\rangle$ is large and the relic density is suppressed.

We evaluate the relic density of higgsinos using Isatools[67] from our scan over NUHM2 parameters as in Sec. 2 and show $\Delta_{\rm EW}$ *vs.* $\Omega_{\widetilde{Z}_1}h^2$ in frame *a*) of Fig. 12. Points with $\Delta_{\rm EW} < 30$ indicative of RNS are shown in red while the more highly fine-tuned points are in blue. The vertical green line shows the WMAP-measured value of the dark matter density. We see that the majority of points with $\Delta_{\rm EW} < 30$ have $\Omega_{\widetilde{Z}_1}h^2 \sim 0.005 - 0.05$, *i.e.* well-below the measured abundance. Several points have $\Omega_{\widetilde{Z}_1}h^2 > 0.12$; these points arise from cases where $\mu \sim M_1$ where the neutralino is of mixed bino-higgsino variety.

There exist a variety of non-standard cosmologies with features which make them more attractive than the standard WIMP-only dark matter scenario. For instance, in stringy models with moduli fields at the 10-100 TeV scale, the moduli may decay after BBN into SM particles, thus diluting all relics present. Alternatively, if moduli decay to SUSY particles which cascade into the LSP, then the neutralino abundance may be enhanced[68].

Another possibility arises from SUSY models where the strong CP problem is solved by the Peccei-Quinn mechanism[69] with its concomitant axion a. In the SUSY case, the axion superfield $\hat{a}$ also contains an R-even spin-0 saxion s and an R-odd spin-$\frac{1}{2}$ axino $\tilde{a}$. In the case where $\widetilde{Z}_1$ is LSP, then the dark matter would be a mixture of two particles: the axion and the neutralino. Axinos which are produced thermally at high re-heat temperature T_R in the early universe would cascade decay to neutralinos at a decay temperature $T_D < T_f$, causing a neutralino *re-annihilation* which provides a much higher abundance of WIMPs than expected in a WIMP-only picture. In addition, saxions can be produced both thermally and via coherent oscillations, and may decay to both SUSY and SM particles: the former case enhances the neutralino abundance while the latter case dilutes any relics present at the time of decay. Calculations of the neutralino abundance in the PQ-augmented MSSM depend on the various PQ parameters along with T_R and the SUSY particle spectrum and have been presented in Ref. [70, 71, 72]. In the case of models with a standard under-abundance of neutralinos, the neutralino abundance is almost always *enhanced* beyond its standard value $\Omega_{\widetilde{Z}_1}h^2$. If this scenario is applied to the case of RNS, then

we may most likely expect an enhanced higgsino-like WIMP abundance beyond its standard value. In this scenario, axions will also be produced via coherent oscillations at temperature around the QCD phase transition. Thus, the higgsinos could make up either a small or a large fraction of the relic dark matter, with axions comprising the remainder. The important point here is that it is very difficult to suppress the higgsino abundance below its standard thermal value which is shown in Fig. 12a). Thus, we would expect relic higgsinos to be present in the universe today, but with an abundance which is suppressed by between $1-15$ from the measured value. This opens up the opportunity to detect relic higgsinos, albeit while these would only constitute a fraction of the measured dark matter abundance. At the same time, there is also the possibility to detect relic axions.

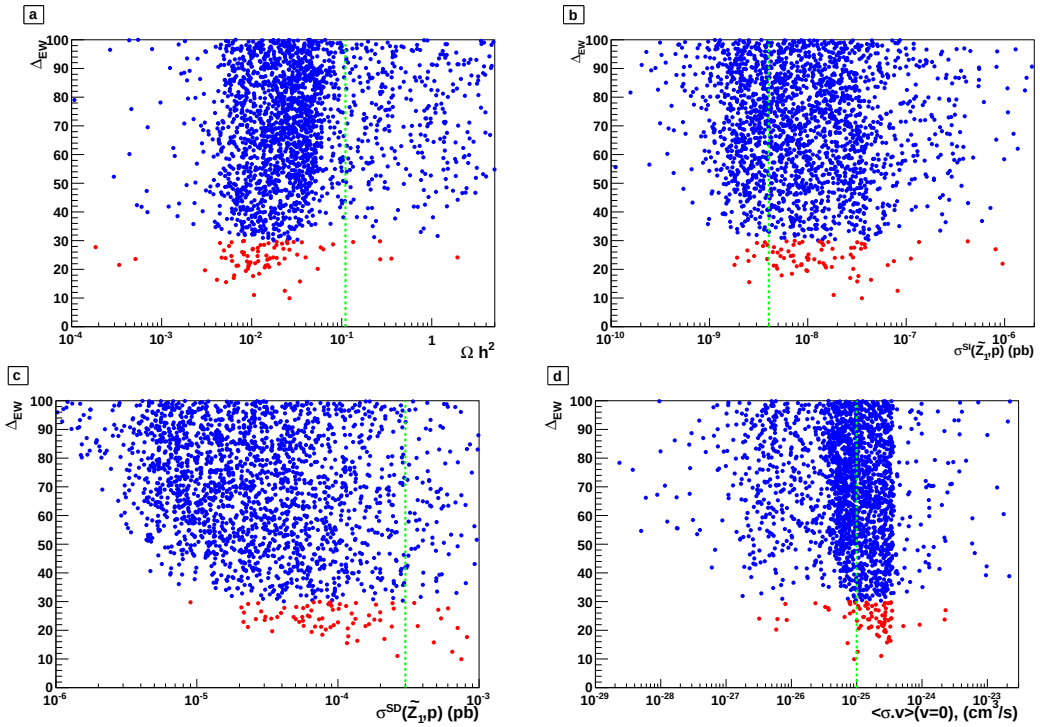

Figure 12: The value of $\Delta_{\rm EW}$ versus neutralino relic density and direct and indirect WIMP detection rates. Vertical green lines denote upper experimental limits obtained assuming that the WIMP saturates the observed density of dark matter. The predictions in the last three frames need to be re-scaled by a factor $\Omega_{\widetilde{Z}_1}h^2/0.11$ if the neutralinos make up only part of the dark matter.

With a view towards detecting relic higgsinos from RNS, we show in Fig. 12b) the value of $\Delta_{\rm EW}$ versus the spin-independent neutralino-proton scattering cross section $\sigma^{SI}(\widetilde{Z}_1 p)$ in pb from Isatools[73]. The red points with $\Delta_{\rm EW} < 30$ occur with $\sigma^{SI}(\widetilde{Z}_1 p) \sim 10^{-9} - 10^{-7}$ pb. For comparison, we show via the green vertical line the Xe-100 limit from 225 live days[74] for $m_{\widetilde{Z}_1} \sim 150$ GeV. Naively, many of the RNS points would be excluded if higgsinos comprised the entire dark matter

density. However, in the mixed axion/higgsino dark matter scenario, the expected local abundance of WIMPs can be scaled down by factors of $1-15$ typically. Even with this rescaling of the expected local abundance, we still expect relic higgsinos to be within detection range of near-future WIMP detectors.

In Fig. 12c), we show the spin-dependent neutralino-proton cross section $\sigma^{SD}(\widetilde{Z}_1 p)$ in pb. The bulk of RNS points with $\Delta_{\rm EW} < 30$ populate the region with $\sigma^{SD}(\widetilde{Z}_1 p) \sim 2\times 10^{-5} - 10^{-3}$ pb. The IceCube neutrino detector at the South Pole is sensitive to detection of neutrinos arising from higgsino annihilation in the core of the sun. The expected detection rate depends on the sun's ability to sweep up neutralinos via $\widetilde{Z}_1 p$ collisions which depends mainly on $\sigma^{SD}(\widetilde{Z}_1 p)$. For reference, we also show the current IceCube WW limit [75] at $\sigma^{SD}(\widetilde{Z}_1 p) \sim 3\times 10^{-4}$ pb. This limit depends on the assumption that WIMPs comprise the entire DM abundance, and would need to be rescaled for a mixed axion/higgsino cosmology.

Fig. 12d) shows the thermally averaged neutralino annihilation cross section times relative velocity, evaluated as $v\to 0$. This quantity enters linearly into indirect searches for neutralino annihilation in the cosmos into γs or e^+, $\bar{p}$ or $\bar{D}$. For the case of RNS, the bulk of points with $\Delta_{\rm EW} < 30$ inhabit the region around $\langle\sigma v\rangle|_{v\to 0} \sim 10^{-25}$ cm^3/sec. The vertical green line shows the upper limit on the annihilation cross section times velocity for very non-relativistic dark matter in dwarf spheroidal satellite galaxies of the Milky Way annihilating to W boson pairs obtained by the Fermi collaboration[76], assuming a ~ 150 GeV WIMP. Models with a larger annihilation cross section would have led to a flux of gamma rays not detected by the experiment, assuming a Navarro-Frenk-White profile[77] for each dwarf galaxy in the analysis. We see that the Fermi bound might exclude the bulk of points assuming higgsinos saturate the DM density. This bound changes rather slowly with the WIMP mass, being just a factor of 2 weaker for a WIMP mass of 300 GeV. Further searches and improvements by the Fermi-LAT Collaboration and/or the impending AMS results should provide more stringent probes of the RNS model.

8. Summary and conclusions

Models of natural supersymmetry reconcile the lack of a SUSY signal at LHC with the principle of electroweak naturalness. Natural SUSY models are characterized by light higgsinos of mass $\sim 100-300$ GeV, three light third generation squarks with mass less than about 500 GeV and gluinos of mass less than about 1.5 TeV. First/second generation squarks may be much heavier – in the multi-TeV regime – thus avoiding LHC searches and providing at least a partial decoupling solution to the SUSY flavor and CP problems. Attractive as they are, generic NS models based on the MSSM are at odds with the recent discovery of a light Higgs scalar at ~ 125 GeV which requires TeV-scale top squarks along with large top-squark mixing.

We presented here an improved natural SUSY model dubbed *radiative natural SUSY* [20], or RNS. RNS is a SUSY model based on the MSSM which may be valid all the way up to the GUT scale. Thus, it maintains the desirable features of gauge coupling unification and radiative electroweak symmetry breaking while avoiding the introduction of extra possibly destabilizing gauge singlets or other forms of exotic matter. The main features of the RNS model include 1) a low value of superpotential higgsino mass $|\mu| \sim 100 - 300$ GeV, and 2) a weak scale value of $-m_{H_u}^2 \sim M_Z^2$: both these qualities are required to fulfill electroweak naturalness at the tree level. The term $m_{H_u}^2$ is driven to low values radiatively by the same mechanism leading to REWSB and depends on a large top quark Yukawa coupling. We proceed further by evaluating EWFT at the 1-loop level. In this case, top squark masses enter the computation of $\Delta_{\rm EW}$ and are also driven radiatively to few-TeV values. By allowing for large top-squark mixing ($|A_0| \sim (1-2)m_0$), top-squark contributions to EWFT are suppressed at the same time as the light Higgs boson mass is uplifted: thus, the model reconciles electroweak fine-tuning with $m_h \simeq 125$ GeV all in the context of the MSSM valid up to the GUT scale.

RNS may be realized in the two-parameter non-universal Higgs models NUHM2. In this case, low EWFT with $\Delta_{\rm EW} \lesssim 30$ can be attained for model parameters which lead to a distinctive mass spectrum:

- light higgsino-like $\widetilde{W}_1$ and $\widetilde{Z}_{1,2}$ with mass $\sim 100 - 300$ GeV,
- gluinos with mass $m_{\tilde{g}} \sim 1 - 4$ TeV,
- heavier top squarks than generic NS models: $m_{\tilde{t}_1} \sim 1 - 2$ TeV and $m_{\tilde{t}_2} \sim 2 - 5$ TeV,
- first/second generation squarks and sleptons with mass $m_{\tilde{q},\tilde{\ell}} \sim 1 - 8$ TeV. The $m_{\tilde{\ell}}$ range can be pushed up to 20-30 TeV if non-universality of generations with $m_0(1,2) > m_0(3)$ is allowed.

The RNS model with the above spectra also fulfills limits from rare B-decay measurements, which can be an Achilles heel for generic NS models with much lighter third generation squarks.

The RNS model can be tested at LHC for $m_{1/2}$ in the lower portion of its range whereupon gluino pair production and/or gaugino pair production may lead to observable signals. Many of the associated SUSY events will contain light higgsinos arising from cascade decays with soft decay products which may be observable. The case of OS/SF dileptons with mass $\lesssim 10 - 20$ GeV would signal the presence of $\widetilde{Z}_2 \to \widetilde{Z}_1 \ell^+ \ell^-$ decay.

Linear e^+e^- colliders would likely provide the definitive test of RNS models since pair production of charged higgsinos should be easily observable and the lowest energy machines will scrutinize the most lucrative parameter choices with the lowest

values of $\Delta_{\rm EW}$. For RNS, an ILC type machine would be a higgsino factory in addition to a Higgs factory.

In RNS, we also expect the presence of higgsino-like WIMPs which have large rates for direct and indirect WIMP detection. Since higgsinos are thermally underproduced, we expect them to constitute only a portion of the measured dark matter abundance, with perhaps axions comprising the remainder. Detectability via WIMP searches will depend on the higgsino fraction of the dark matter.

The many elegant features presented above impel us to regard RNS as the possible new paradigm SUSY model. Its consequences for detection at colliders and at dark matter detectors merits a high level of scrutiny.

Acknowledgments

We thank Javier Ferrandis for various calculations concerning the effective potential. This work was supported in part by the U.S. Department of Energy.

A. Radiative corrections to the Higgs potential minimization conditions

The Higgs portion of the scalar potential in the MSSM is given by

$$V_{Higgs} = V_{\rm tree} + \Delta V, \tag{A.1}$$

where the tree level portion for the neutral Higgs sector is given by

$$\begin{aligned} V_{\rm tree} &= (m_{H_u}^2 + \mu^2)|h_u^0|^2 + (m_{H_d}^2 + \mu^2)|h_d^0|^2 \\ &-B\mu(h_u^0 h_d^0 + h.c.) + \frac{1}{8}(g^2 + g'^2)(|h_u^0|^2 - |h_d^0|^2)^2 \end{aligned} \tag{A.2}$$

and the radiative corrections (in the effective potential approximation, and using the $\overline{DR}$ regularization scheme, as appropriate for SUSY models) by

$$\Delta V = \sum_i \frac{(-1)^{2s_i}}{64\pi^2}(2s_i+1)c_i m_i^4 \left[\log\left(\frac{m_i^2}{Q^2}\right) - \frac{3}{2}\right], \tag{A.3}$$

where the sum over i runs over all fields that couple to Higgs fields, m_i^2 are the *Higgs field dependent* mass squared values, and $c_i = c_{col}c_{cha}$, with $c_{col} = 3$ (1) for colored (uncolored) particles and $c_{cha} = 2$ (1) for charged (neutral) particles and s_i is their spin quantum number.

Minimization of the scalar potential allows one to compute the gauge boson masses in terms of the Higgs field vacuum expectation values v_u and v_d, and leads to the well-known conditions that

$$B\mu v_d = \left(m_{H_u}^2 + \mu^2 - g_Z^2(v_d^2 - v_u^2)\right) v_u + \Sigma_u \tag{A.4}$$

$$B\mu v_u = \left(m_{H_d}^2 + \mu^2 + g_Z^2(v_d^2 - v_u^2)\right) v_d + \Sigma_d\,, \tag{A.5}$$

where

$$\Sigma_{u,d} = \frac{\partial \Delta V}{\partial h_{u,d}}\Big|_{min} \tag{A.6}$$

and $h^0_{u,d} = (h^0_{u,dR} + i h^0_{u,dI})/\sqrt{2}$, $g_Z^2 = (g^2 + g'^2)/8$. By $SU(2)$ invariance, the scalar potential V depends on the scalar fields as [6] $V(h_u^\dagger h_u, h_d^\dagger h_d, h_u h_d + \text{c.c.})$, then we have

$$\Sigma_u = \Sigma_u^u v_u + \Sigma_u^d v_d\,, \tag{A.7}$$

$$\Sigma_d = \Sigma_d^u v_u + \Sigma_d^d v_d \quad \text{and} \tag{A.8}$$

$$\Sigma_d^u = \Sigma_u^d \tag{A.9}$$

where

$$\Sigma_u^u = \frac{\partial \Delta V}{\partial |h_u|^2}\Big|_{min}, \tag{A.10}$$

$$\Sigma_d^d = \frac{\partial \Delta V}{\partial |h_d|^2}\Big|_{min} \quad \text{and} \tag{A.11}$$

$$\Sigma_u^d = \frac{\partial \Delta V}{\partial (h_u h_d + \text{c.c.})}\Big|_{min}. \tag{A.12}$$

In this case, the minimization conditions may be expressed as

$$M_Z^2/2 = \frac{(m_{H_d}^2 + \Sigma_d^d) - (m_{H_u}^2 + \Sigma_u^u)\tan^2\beta}{\tan^2\beta - 1} - \mu^2, \tag{A.13}$$

$$B\mu = \left((m_{H_u}^2 + \mu^2 + \Sigma_u^u) + (m_{H_d}^2 + \mu^2 + \Sigma_d^d)\right)\sin\beta\cos\beta + \Sigma_u^d. \tag{A.14}$$

The advantage of writing the minimization conditions in terms of Σ_u^u and Σ_d^d and Σ_{ud} is that the corrections to $m_{H_u}^2$, $m_{H_d}^2$ and $B\mu$ are neatly separated so that Σ_u^d terms do not appear in Eq. (A.13), and so do not contribute to the fine-tuning calculation.

The contributions of the various Σs can be written as:

$$\begin{aligned}
\Sigma_u^u &= \sum_i \frac{1}{32\pi^2}(-1)^{2s_i}(2s_i+1)c_i \frac{\partial m_i^2}{\partial |h_u|^2}\Big|_{min} F(m_i^2)\,, \\
\Sigma_d^d &= \sum_i \frac{1}{32\pi^2}(-1)^{2s_i}(2s_i+1)c_i \frac{\partial m_i^2}{\partial |h_d|^2}\Big|_{min} F(m_i^2)\,, \\
\Sigma_u^d &= \sum_i \frac{1}{32\pi^2}(-1)^{2s_i}(2s_i+1)c_i \frac{\partial m_i^2}{\partial (h_u h_d + \text{c.c.})}\Big|_{min} F(m_i^2) = \Sigma_d^u.
\end{aligned} \tag{A.15}$$

where

$$F(m^2) = m^2\left(\log\frac{m^2}{Q^2} - 1\right). \tag{A.16}$$

with the optimized scale choice $Q^2 = m_{\tilde{t}_1} m_{\tilde{t}_2}$.

For the top squark contributions, we find

$$\Sigma_u^u(\tilde{t}_{1,2}) = \frac{3}{16\pi^2} F(m^2_{\tilde{t}_{1,2}}) \left[f_t^2 - g_Z^2 \mp \frac{f_t^2 A_t^2 - 8g_Z^2(\frac{1}{4} - \frac{2}{3}x_W)\Delta_t}{m^2_{\tilde{t}_2} - m^2_{\tilde{t}_1}} \right] \tag{A.17}$$

$$\Sigma_d^d(\tilde{t}_{1,2}) = \frac{3}{16\pi^2} F(m^2_{\tilde{t}_{1,2}}) \left[g_Z^2 \mp \frac{f_t^2 \mu^2 + 8g_Z^2(\frac{1}{4} - \frac{2}{3}x_W)\Delta_t}{m^2_{\tilde{t}_2} - m^2_{\tilde{t}_1}} \right] \tag{A.18}$$

where $\Delta_t = (m^2_{\tilde{t}_L} - m^2_{\tilde{t}_R})/2 + M_Z^2 \cos 2\beta(\frac{1}{4} - \frac{2}{3}x_W)$ and $x_W \equiv \sin^2\theta_W$. In the denominator of (A.17) and (A.18), the tree level expressions of $m^2_{\tilde{t}_{1,2}}$ should be used.

For b-squark contributions, we have

$$\Sigma_u^u(\tilde{b}_{1,2}) = \frac{3}{16\pi^2} F(m^2_{\tilde{b}_{1,2}}) \left[g_Z^2 \mp \frac{f_b^2 \mu^2 - 8g_Z^2(\frac{1}{4} - \frac{1}{3}x_W)\Delta_b}{m^2_{\tilde{b}_2} - m^2_{\tilde{b}_1}} \right]$$

$$\Sigma_d^d(\tilde{b}_{1,2}) = \frac{3}{16\pi^2} F(m^2_{\tilde{b}_{1,2}}) \left[f_b^2 - g_Z^2 \mp \frac{f_b^2 A_b^2 - 8g_Z^2(\frac{1}{4} - \frac{1}{3}x_W)\Delta_b}{m^2_{\tilde{b}_2} - m^2_{\tilde{b}_1}} \right] \tag{A.19}$$

where $\Delta_b = (m^2_{\tilde{b}_L} - m^2_{\tilde{b}_R})/2 - M_Z^2 \cos 2\beta(\frac{1}{4} - \frac{1}{3}x_W)$. The expressions for $\Sigma_u^u(\tilde{\tau}_{1,2})$ and $\Sigma_d^d(\tilde{\tau}_{1,2})$ are similar to $\Sigma_u^u(\tilde{b}_{1,2})$ and $\Sigma_d^d(\tilde{b}_{1,2})$ but with $b \to \tau$, $c_{col} = 1$ and $(\frac{1}{4} - \frac{1}{3}x_W) \to (\frac{1}{4} - x_W)$.

For first/second generation sfermion contributions, we find

$$\Sigma_{u,d}^{u,d}(\tilde{f}_{L,R}) = \frac{c_{col}}{16\pi^2} F(m^2_{\tilde{f}_{L,R}}) \left(4g_Z^2(T_3 - Qx_W\right) \tag{A.20}$$

where T_3 is the weak isospin and Q is the electric charge assignment (taking care to flip the sign of Q for R-sfermions). For instance,

$$\Sigma_u^u(\tilde{u}_L) = \frac{3}{16\pi^2} F(m^2_{\tilde{u}_L}) \left(f_u^2 - 4g_Z^2(\frac{1}{2} - \frac{2}{3}x_W) \right) \tag{A.21}$$

$$\Sigma_u^u(\tilde{u}_R) = \frac{3}{16\pi^2} F(m^2_{\tilde{u}_R}) \left(f_u^2 - 4g_Z^2(\frac{2}{3}x_W) \right) \tag{A.22}$$

$$\Sigma_d^d(\tilde{u}_L) = \frac{3}{16\pi^2} F(m^2_{\tilde{u}_L}) \left(4g_Z^2(\frac{1}{2} - \frac{2}{3}x_W) \right) \tag{A.23}$$

$$\Sigma_d^d(\tilde{u}_R) = \frac{3}{16\pi^2} F(m^2_{\tilde{u}_R}) \left(4g_Z^2(\frac{2}{3}x_W) \right). \tag{A.24}$$

These contributions, arising from electroweak D-term contributions to masses, cancel out separately for squarks and sleptons in the limit of mass degeneracy, due to the fact that weak isospins and electric charges (or weak hypercharges) sum to zero in each generation. For this reason, we sum these contributions before taking the maximum contribution to the fine-tuning measure $\Delta_{\rm EW}$.

For chargino contributions, we find

$$\Sigma_u^u(\widetilde{W}_{1,2}^{\pm}) = \frac{-g^2}{16\pi^2} F(m^2_{\widetilde{W}_{1,2}}) \left(1 \mp \frac{M_2^2 + \mu^2 - 2m_W^2 \cos 2\beta}{m^2_{\widetilde{W}_2} - m^2_{\widetilde{W}_1}}\right) \tag{A.25}$$

$$\Sigma_d^d(\widetilde{W}_{1,2}^{\pm}) = \frac{-g^2}{16\pi^2} F(m^2_{\widetilde{W}_{1,2}}) \left(1 \mp \frac{M_2^2 + \mu^2 + 2m_W^2 \cos 2\beta}{m^2_{\widetilde{W}_2} - m^2_{\widetilde{W}_1}}\right). \tag{A.26}$$

For contributions from neutralinos, we find[5]

$$\Sigma_u^u(\widetilde{Z}_i) = \frac{1}{16\pi^2} \frac{F(m^2_{\widetilde{Z}_i})}{D(\widetilde{Z}_i)} \left[K(\widetilde{Z}_i) - 2(g^2 + g'^2)\mu^2 M_Z^2 \cos^2\beta (m^2_{\widetilde{Z}_i} - m^2_{\tilde{\gamma}})\right], \tag{A.27}$$

$$\Sigma_d^d(\widetilde{Z}_i) = \frac{1}{16\pi^2} \frac{F(m^2_{\widetilde{Z}_i})}{D(\widetilde{Z}_i)} \left[K(\widetilde{Z}_i) - 2(g^2 + g'^2)\mu^2 M_Z^2 \sin^2\beta (m^2_{\widetilde{Z}_i} - m^2_{\tilde{\gamma}})\right], \tag{A.28}$$

where

$$\begin{aligned} K(\widetilde{Z}_i) = & -m^6_{\widetilde{Z}_i}(g^2 + g'^2) \\ & + m^4_{\widetilde{Z}_i}\left[g^2(M_1^2 + \mu^2) + g'^2(M_2^2 + \mu^2) + (g^2 + g'^2)M_Z^2\right] \\ & - m^2_{\widetilde{Z}_i}\left[\mu^2(g^2 M_1^2 + g'^2 M_2^2) + (g^2 + g'^2)M_Z^2 m^2_{\tilde{\gamma}}\right], \end{aligned} \tag{A.29}$$

$D(\widetilde{Z}_i) = \prod_{j\neq i}(m^2_{\widetilde{Z}_i} - m^2_{\widetilde{Z}_j})$, and $m_{\tilde{\gamma}} = M_1 \cos^2\theta_W + M_2 \sin^2\theta_W$. Our neutralino corrections differ in form as well as numerically from those in the literature where these were calculated using the neutralino mass (not mass squared) matrix [39, 40].

For weak bosons, we find

$$\Sigma_u^u(W^{\pm}) = \Sigma_d^d(W^{\pm}) = \frac{3g^2}{32\pi^2} F(m_W^2) \tag{A.30}$$

$$\Sigma_u^u(Z^0) = \Sigma_d^d(Z^0) = \frac{3g^2}{64\pi^2 \cos^2\theta_W} F(M_Z^2). \tag{A.31}$$

For Higgs bosons, we find

$$\Sigma_u^u(h, H) = \frac{g_Z^2}{16\pi^2} F(m^2_{h,H}) \left(1 \mp \frac{M_Z^2 + m_A^2(1 + 4\cos 2\beta + 2\cos^2 2\beta)}{m_H^2 - m_h^2}\right), \tag{A.32}$$

$$\Sigma_d^d(h, H) = \frac{g_Z^2}{16\pi^2} F(m^2_{h,H}) \left(1 \mp \frac{M_Z^2 + m_A^2(1 - 4\cos 2\beta + 2\cos^2 2\beta)}{m_H^2 - m_h^2}\right) \tag{A.33}$$

and

[5]Unlike the case of other contributions where it is easy to explicitly find the eigenvalues of the Higgs-field-dependent squared mass matrices, this is not possible for the neutralino. To evaluate the derivatives of the eigenvalues of the *squared* neutralino mass matrix that appear in (A.15), we use the technique introduced in Ref. [39] and elaborated further in Ref. [78].

$$\Sigma_u^u(H^\pm) = \Sigma_d^d(H^\pm) = \frac{g^2}{32\pi^2} F(m_{H^\pm}^2). \tag{A.34}$$

For SM fermions t, b and τ, we find

$$\Sigma_u^u(t) = -\frac{3f_t^2}{8\pi^2} F(m_t^2), \tag{A.35}$$

$$\Sigma_d^d(t) = 0 \tag{A.36}$$

$$\Sigma_u^u(b) = 0, \tag{A.37}$$

$$\Sigma_d^d(b) = -\frac{3f_b^2}{8\pi^2} F(m_b^2) \tag{A.38}$$

$$\Sigma_u^u(\tau) = 0, \tag{A.39}$$

$$\Sigma_d^d(\tau) = -\frac{f_\tau^2}{8\pi^2} F(m_\tau^2). \tag{A.40}$$

References

[1] G. Aad *et al.* [ATLAS Collaboration], *Phys. Lett.* **B 716** (2012) 1.

[2] S. Chatrchyan *et al.* [CMS Collaboration], *Phys. Lett.* **B 716** (2012) 30.

[3] M. S. Carena and H. E. Haber, *Prog. Part. Nucl. Phys.* **50** (2003) 63 [hep-ph/0208209].

[4] G. Aad *et al.* [ATLAS Collaboration], Phys. Rev. D **87** (2013) 012008.

[5] S. Chatrchyan *et al.* [CMS Collaboration], *J. High Energy Phys.* **1210** (2012) 018.

[6] H. Baer and X. Tata, *Weak Scale Supersymmetry: From Superfields to Scattering Events*, (Cambridge University Press, 2006); M. Drees, R. Godbole and P. Roy, *Theory and Phenomenology of Sparticles*, (World Scientific, 2004); P. Binetruy, *Supersymmetry*, (Oxford University Press, 2006); S. P. Martin, hep-ph/9709356.

[7] E. Witten, *Nucl. Phys.* **B 188** (1981) 513; N. Sakai, *Z. Physik* **C 11** (1981) 153; S. Dimopoulos and H. Georgi, *Nucl. Phys.* **B 193** (1981) 150; R. Kaul, *Phys. Lett.* **B 109** (1982) 19.

[8] R. Kitano and Y. Nomura, *Phys. Lett.* **B 631** (2005) 58; *Phys. Rev.* **D 73** (2006) 095004; hep-ph/0606134.

[9] N. Arkani-Hamed, talk at WG2 meeting, Oct. 31, 2012, CERN, Geneva.

[10] M. Papucci, J. T. Ruderman and A. Weiler, *J. High Energy Phys.* **1209** (2012) 035; C. Brust, A. Katz, S. Lawrence and R. Sundrum, *J. High Energy Phys.* **1203** (2012) 103; R. Essig, E. Izaguirre, J. Kaplan and J. G. Wacker, *J. High Energy Phys.* **1201** (2012) 074; C. Wymant, *Phys. Rev.* **D 86** (2012) 115023; E. Arganda, J. L. Diaz-Cruz and A. Szynkman, European Physical Journal C **73** (2013) 2384.

[11] H. Baer, V. Barger, P. Huang and X. Tata, *J. High Energy Phys.* **1205** (2012) 109.

[12] H. Baer, V. Barger and A. Mustafayev, *Phys. Rev.* **D 85** (2012) 075010.

[13] L. Hall, D. Pinner and J. T. Ruderman, *J. High Energy Phys.* **1204** (2012) 131.

[14] H. Baer, V. Barger and P. Huang, *J. High Energy Phys.* **1111** (2011) 031.

[15] S. F. King, M. Muhlleitner and R. Nevzorov, Higgs Benchmarks Near 125 GeV," *Nucl. Phys.* **B 860** (2012) 207; J. F. Gunion, Y. Jiang and S. Kraml, 125 GeV," *Phys. Lett.* **B 710** (2012) 454; K. J. Bae, K. Choi, E. J. Chun, S. H. Im, C. B. Park and C. S. Shin, *J. High Energy Phys.* **1211** (2012) 118, `arXiv:1208.2555` [hep-ph]; J. Cao, Z. Heng, J. M. Yang, Y. Zhang, J. Zhu, *J. High Energy Phys.* **1203** (2012) 086, arXiv:1202.5821 [hep-ph].

[16] K. S. Babu, I. Gogoladze, M. U. Rehman and Q. Shafi, *Phys. Rev.* **D 78** (2008) 055017; S. P. Martin, *Phys. Rev.* **D 81** (2010) 035004 and *Phys. Rev.* **D 82** (2010) 055019; K. J. Bae, T. H. Jung and H. D. Kim, in supersymmetry with vector-like matters," *Phys. Rev.* **D 87** (2013) 015014, `arXiv:1208.3748` [hep-ph].

[17] J. Bagger, E. Poppitz and L. Randall, *Nucl. Phys.* **B 455** (1995) 59.

[18] R. Barbieri and G. Giudice, *Nucl. Phys.* **B 306** (1988) 63.

[19] J. R. Ellis, K. Enqvist, D. V. Nanopoulos and F. Zwirner, Mod. Phys. Lett. A **1** (1986) 57.

[20] H. Baer, V. Barger, P. Huang, A. Mustafayev and X. Tata, *Phys. Rev. Lett.* **109** (2012) 161802; H. Baer, `arXiv:1210.7852`.

[21] S. Weinberg, *Phys. Rev. Lett.* **48** (1982) 1303; M. Khlopov and A. Linde, *Phys. Lett.* **B 138** (1984) 265.

[22] M. Kawasaki, K. Kohri, T. Moroi and A. Yotsuyanagi, *Phys. Rev.* **D 78** (2008) 065011.

[23] G. Aad *et al.* [ATLAS Collaboration], Phys. Lett. B **720** (2013) 13.

[24] J. A. Casas, J. R. Espinosa and I. Hidalgo, JHEP **0401** (2004) 008.

[25] H. Baer, F. E. Paige, S. D. Protopopescu and X. Tata, `hep-ph/9305342`; A. Djouadi, J. -L. Kneur and G. Moultaka, Comput. Phys. Commun. **176** (2007) 426; J. Conley, S. Gainer, J. Hewett, M. Le and T. Rizzo, *Eur. Phys. J.* **C 71** (2011) 1697;

S. Sekmen, S. Kraml, J. Lykken, F. Moortgat, S. Padhi, L. Pape, M. Pierini and H. B. Prosper *et al.*, *J. High Energy Phys.* **1202** (2012) 075; M. W. Cahill-Rowley, J. L. Hewett, A. Ismail and T. G. Rizzo, `arXiv:1211.1981` [hep-ph].

[26] K. L. Chan, U. Chattopadhyay and P. Nath, *Phys. Rev.* **D 58** (1998) 096004; J. Feng, K. Matchev and T. Moroi, *Phys. Rev. Lett.* **84** (2000) 2322 and *Phys. Rev.* **D 61** (2000) 075005; J. L. Feng, K. T. Matchev and F. Wilczek, *Phys. Lett.* **B 482** (2000) 388; J. L. Feng and F. Wilczek, *Phys. Lett.* **B 631** (2005) 170; J. L. Feng, K. T. Matchev and D. Sanford, *Phys. Rev.* **D 85** (2012) 075007; J. L. Feng and D. Sanford, *Phys. Rev.* **D 86** (2012) 055015; this low μ region of mSUGRA had already been noted in, H. Baer, C. H. Chen, F. Paige and X. Tata, *Phys. Rev.* **D 52** (1995) 2746 and *Phys. Rev.* **D 53** (1996) 6241; H. Baer, C. H. Chen, M. Drees, F. Paige and X. Tata, *Phys. Rev.* **D 59** (1999) 055014; the phenomenology of this region is discussed in H. Baer, T. Krupovnickas, S. Profumo and P. Ullio, *J. High Energy Phys.* **0510** (2005) 020.

[27] H. Baer, V. Barger, P. Huang, D. Mickelson, A. Mustafayev and X. Tata, *Phys. Rev.* **D 87** (2013) 035017 `arXiv:1210.3019`.

[28] H. Baer, V. Barger and A. Mustafayev, *J. High Energy Phys.* **1205** (2012) 091.

[29] H. Baer, A. Mustafayev, H. Summy and X. Tata, *J. High Energy Phys.* **0710** (2007) 088.

[30] H. Baer, A. Mustafayev, E. -K. Park, S. Profumo and X. Tata, *J. High Energy Phys.* **0604** (2006) 041.

[31] For further work on non-universal gaugino masses, see I. Gogoladze, F. Nasir and Q. Shafi, arXiv:1212.2593 [hep-ph].

[32] J. Ellis, K. Olive and Y. Santoso, *Phys. Lett.* **B 539** (2002) 107; J. Ellis, T. Falk, K. Olive and Y. Santoso, *Nucl. Phys.* **B 652** (2003) 259; H. Baer, A. Mustafayev, S. Profumo, A. Belyaev and X. Tata, *J. High Energy Phys.* **0507** (2005) 065.

[33] G. F. Giudice and A. Masiero, *Phys. Lett.* **B 206** (1988) 480.

[34] H. Baer, A. Mustafayev, S. Profumo, A. Belyaev and X. Tata, *Phys. Rev.* **D 71** (2005) 095008.

[35] K. Choi, K. S. Jeong, T. Kobayashi and K. -i. Okumura, *Phys. Lett.* **B 633** (2006) 355; O. Lebedev, H. P. Nilles and M. Ratz, `hep-ph/0511320`; K. Choi, K. S. Jeong, T. Kobayashi and K. -i. Okumura, *Phys. Rev.* **D 75** (2007) 095012; M. Badziak *et al.* `arXiv:1212.0854` [hp-ph]

[36] S. Antusch, L. Calibbi, V. Maurer, M. Monaco and M. Spinrath, JHEP **01** (2013) 187;

[37] J. Feng, K. Matchev and T. Moroi, Ref.[26].

[38] L. E. Ibañez and G. G. Ross, Phys. Lett. **B110**, 215 (1982); K. Inoue *et al.* Prog. Theor. Phys. **68**, 927 (1982) and **71**, 413 (1984); L. Ibañez, Phys. Lett. **B118**, 73 (1982); J. Ellis, J. Hagelin, D. Nanopoulos and M. Tamvakis, Phys. Lett. **B125**, 275 (1983); L. Alvarez-Gaumé. J. Polchinski and M. Wise, Nucl. Phys. **B221**, 495 (1983).

[39] R. Arnowitt and P. Nath, *Phys. Rev.* **D 46** (1992) 3981.

[40] A. V. Gladyshev, D. I. Kazakov, W. de Boer, G. Burkart and R. Ehret, *Nucl. Phys.* **B 498** (1997) 3.

[41] R. Aaij *et al.* [LHCb Collaboration], Phys. Rev. Lett. **110** (2013) 021801

[42] F. Gabbiani, E. Gabrielli, A. Masiero and L. Silvestrini, general SUSY extensions *Nucl. Phys.* **B 477** (1996) 321.

[43] J. Hagelin, S. Kelley and T. Tanaka, *Nucl. Phys.* **B 415** (1994) 293; H. Baer, A. Belyaev, T. Krupovnickas and A. Mustafayev, *J. High Energy Phys.* **0406** (2004) 044.

[44] ISAJET, by H. Baer, F. Paige, S. Protopopescu and X. Tata, `hep-ph/0312045`.

[45] H. Baer, C. H. Chen, R. Munroe, F. Paige and X. Tata, *Phys. Rev.* **D 51** (1995) 1046; H. Baer, J. Ferrandis, S. Kraml and W. Porod, *Phys. Rev.* **D 73** (2006) 015010.

[46] J. Hisano, H. Murayama, and T. Yanagida, *Nucl. Phys.* **B 402** (1993) 46; Y. Yamada, *Z. Physik* **C 60** (1993) 83 ; J. L. Chkareuli and I. G. Gogoladze, *Phys. Rev.* **D 58** (1998) 055011.

[47] S. Martin and M. Vaughn, *Phys. Rev.* **D 50** (1994) 2282.

[48] Y. Yamada, *Phys. Lett.* **B 316** (1993) 109; *Phys. Rev. Lett.* **72** (1994) 25; *Phys. Rev.* **D 50** (1994) 3537.

[49] H. Haber and R. Hempfling, *Phys. Rev.* **D 48** (1993) 4280.

[50] D. Pierce, J. Bagger, K. Matchev and R. Zhang, *Nucl. Phys.* **B 491** (1997) 3.

[51] Joint LEP 2 Supersymmetry Working Group, *Combined LEP Chargino Results up to 208 GeV*, `http://lepsusy.web.cern.ch/lepsusy/www/inos_moriond01/charginos_pub.html`.

[52] N. Arkani-Hamed and H. Murayama, *Phys. Rev.* **D 56** (1997) 6733.

[53] K. Agashe and M. Graesser, *Phys. Rev.* **D 59** (1998) 015007.

[54] H. Baer, C. Balazs, P. Mercadante, X. Tata and Y. Wang, *Phys. Rev.* **D 63** (2001) 015011.

[55] H. Baer, V. Barger, A. Lessa and X. Tata, *J. High Energy Phys.* **1006** (2010) 102, *Phys. Rev.* **D 85** (2012) 051701 and *Phys. Rev.* **D 86** (2012) 117701.

[56] H. Baer, A. Belyaev, T. Krupovnickas and X. Tata, *J. High Energy Phys.* **0402** (2004) 007; H. Baer, T. Krupovnickas and X. Tata, *J. High Energy Phys.* **0406** (2004) 061.

[57] D. Asner *et al.* [Heavy Flavor Averaging Group], `arXiv:1010.1589` [hep-ex].

[58] M. Misiak *et al.*, *Phys. Rev. Lett.* **98** (2007) 022002.

[59] H. Baer and M. Brhlik, *Phys. Rev.* **D 55** (1997) 3201.

[60] G. Buchalla, A. J. Buras and M. Lautenbacher, Rev. Mod. Phys. **68** (1996) 1125.

[61] S. Rai Choudhury and N. Gaur, *Phys. Lett.* **B 451** (1998) 86; K. S. Babu and C. F. Kolda, *Phys. Rev.* **D 84** (2000) 28; our calculation uses the formulae in J. Mizukoshi, X. Tata and Y. Wang, *Phys. Rev.* **D 66** (2002) 115003.

[62] H. Baer, S. Kraml and S. Kulkarni, *J. High Energy Phys.* **1212** (2012) 066, `arXiv:1208.3039` [hep-ph].

[63] G. W. Bennett *et al.* (Muon $g-2$ Collaboration), *Phys. Rev.* **D 80** (2009) 052008.

[64] H. Baer, V. Barger, P. Huang, D. Mickelson, A. Mustafayev, W. Sreethawong and X. Tata, in preparation.

[65] H. Baer, V. Barger, S. Kraml, A. Lessa, W. Sreethawong and X. Tata, JHEP **1203** (2012) 092.

[66] H. Baer, V. Barger, A. Lessa, W. Sreethawong and X. Tata, Phys. Rev. D **85** (2012) 055022.

[67] IsaReD, see H. Baer, C. Balazs and A. Belyaev, *J. High Energy Phys.* **0203** (2002) 042.

[68] T. Moroi and L. Randall, *Nucl. Phys.* **B 570** (2000) 455; G. Gelmini and P. Gondolo, *Phys. Rev.* **D 74** (2006) 023510; G. Gelmini, P. Gondolo, A. Soldatenko and C. Yaguna, *Phys. Rev.* **D 74** (2006) 083514; G. Gelmini, P. Gondolo, A. Soldatenko and C. Yaguna, *Phys. Rev.* **D 76** (2007) 015010; B. Acharya, K. Bobkov, G. Kane, P. Kumar and J. Shao, *Phys. Rev.* **D 76** (2007) 126010 and *Phys. Rev.* **D 78** (2008) 065038; B. Acharya, P. Kumar, K. Bobkov, G. Kane, J. Shao and S. Watson, *J. High Energy Phys.* **0806** (2008) 064; R. Allahverdi, B. Dutta and K. Sinha, Phys. Rev. D **86** (2012) 095016.

[69] R. Peccei and H. Quinn, *Phys. Rev. Lett.* **38** (1977) 1440 and *Phys. Rev.* **D 16** (1977) 1791; S. Weinberg, *Phys. Rev. Lett.* **40** (1978) 223; F. Wilczek, *Phys. Rev. Lett.* **40** (1978) 279; J. E. Kim, *Phys. Rev. Lett.* **43** (1979) 103; M. A. Shifman, A. Vainstein and V. I. Zakharov, *Nucl. Phys.* **B 166** (1980) 493; M. Dine, W. Fischler and M. Srednicki, *Phys. Lett.* **B 104** (1981) 199; A. P. Zhitnitskii, *Sov. J. Nucl.* **31** (1980) 260.

[70] K-Y. Choi, J. E. Kim, H. M. Lee and O. Seto, *Phys. Rev.* **D 77** (2008) 123501.

[71] H. Baer, A. Lessa, S. Rajagopalan and W. Sreethawong, JCAP**1106** (2011) 031.

[72] H. Baer, A. Lessa and W. Sreethawong, JCAP**1201** (2012) 036.

[73] H. Baer, C. Balazs, A. Belyaev and J. O'Farrill, JCAP **0309** (2003) 007.

[74] E. Aprile *et al.* [XENON100 Collaboration], *Phys. Rev. Lett.* **109** (2012) 181301.

[75] R. Abbasi *et al.* (IceCube collaboration), *Phys. Rev.* **D 85** (2012) 042002.

[76] M. Ackermann *et al.* (Fermi Collaboration), *Phys. Rev. Lett.* **107** (2011) 241302; A. Geringer-Sameth and S. M. Koushiappas, *Phys. Rev. Lett.* **107** (2011) 241303.

[77] J. Navarro, C. S. Frenk and S. White, *Astrophys. J.* **462** (1996) 563.

[78] T. Ibrahim and P. Nath, *Phys. Rev.* **D 66** (2002) 015005.